BRIGHAM YOUNG UNIVERSITY

GEOLOGY STUDIES

Volume 17 Part 1 May 1970

CONTENTS

Brigham Young University Geology Studies

Volume 17, Part 1 — May 1970

Contents

A publication of the
Department of Geology
Brigham Young University
Provo, Utah 84601

Editor

J. Keith Rigby

Brigham Young University Geology Studies is published semi-annually by the department. *Geology Studies* consists of graduate student and staff research in the department and occasional papers from other contributors, and is the successor to *BYU Research Studies, Geology Series,* published in separate numbers from 1954 to 1960.

Distributed June 5, 1970

Price $3.00

Lateral and Vertical Variations in a Quaternary Basalt Flow: Petrography and Chemistry of the Gunlock Flow, Southwestern Utah

GLENN F. EMBREE
Ricks College, Rexburg, Idaho

ABSTRACT.—Lateral chemical variation in the Gunlock flow is insignificant. Vertically there is a decrease in SiO_2, Na_2O, K_2O, MgO, FeO, U, and Th and an increase in CaO near the top of the flow; CaO, MgO, and FeO locally show a minimum near the center, and Na_2O, K_2O, U and SiO_2 possibly decrease near the base. Although modal variations are slight and mostly inconsistent, plagioclase appears to decrease upward. Flowage differentiation, post-emplacement volatile escape of alkalies and SiO_2, and differential diffusion of ions in the melt are possible causes of the observed chemical and modal variations. Primary oxidation of Fe-Ti oxides is most intense in the lower two-thirds of the flow and reflects temperature distribution in the cooling flow. Stability fields of rutile-titanohematite and rutile-pseudobrookite-titanohematite exist at approximately 700°C.

For comparative compositional studies at least 3 samples should be taken from each of several widely spaced vertical sections to overcome the effect of intraflow variation.

CONTENTS

TEXT

ILLUSTRATIONS

INTRODUCTION

The question of how much and what type of variation exists within a single basalt flow has been brought about by the enormous quantity of recent work being done on these rocks. Interflow and interregional comparisons of basalt compositions require the determination of chemical or mineralogical variations that might be present within a single flow. If significant variation does exist, these comparative studies could be misleading if representative sampling techniques are not used.

Purpose

The purposes of this study are to (a) determine the nature of vertical and lateral variations in mineralogical and chemical composition found within a single basalt flow within the extensive Late Cenozoic volcanic field of southwestern Utah and northwestern Arizona, and (b) define and interpret the trends in this variation. The Gunlock flow, located approximately 15 miles northwest of St. George, Utah, (Text-fig. 1) was chosen for this study because of its generally good exposure (Plate 2) and accessibility. Coincidentally, it is intermediate, relative to some elemental concentrations, between flows in the western Grand Canyon region (Best, *et al.*, 1969) as well as in world wide averages for tholeiites and alkali olivine basalts.

Method of Study

The extent of the Gunlock flow, as well as its spatial and temporal relationships to other flows in the area, was first determined by mapping on aerial photographs of scale 1:20,000. Samples were taken at approximately 3 foot intervals in 7 vertical sections located approximately one mile apart along the length of the flow (Plate 1). In the tables and figures which follow, samples are keyed to a vertical section and the height, in feet, above the base of the flow; thus, 3-6 refers to a sample collected six feet above the base of the flow in section 3. Fifty-nine samples were analyzed for major elements as well as for U, Th, and Ti by atomic absorption and gamma-ray spectrometry. The FeO and total Fe contents for some samples from one section were determined by Dr. A.G. Loomis as an independent check on accuracy and as an evaluation of

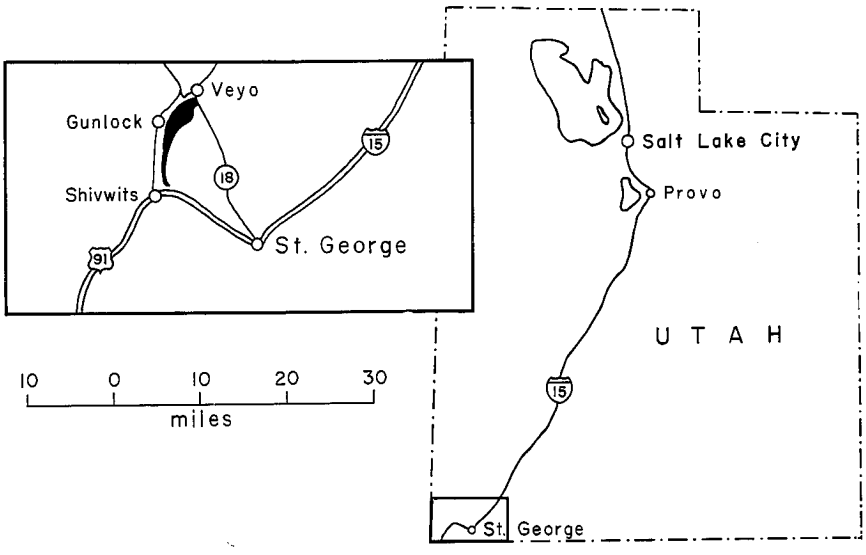

TEXT-FIGURE 1.—Index map of the Gunlock area in Washington County, Utah. The area mapped is in black.

oxidation variation. Thin sections were prepared from all samples from two sections in order to determine modal and textural variations. Variations in the oxide phases present were determined by X-ray diffraction and polished section studies.

Previous Work

Areal mapping of lithologic units in this and adjacent areas has been done by Cook (1957, 1960), McCarthy (1959), and Wiley (1963), but they did not differentiate the basaltic rocks into individual flows or describe them in any detail. Hamblin (1963) established a chronological classification of the basalts in the St. George area and has since expanded this system of classification to include the basalts of northwest Arizona and adjacent Utah (Best, *et al.*, 1969). Best and Brimhall (see Best, *et al.*, 1969) have undertaken a detailed study of the chemical and mineralogical variation of the basaltic rocks in the western Grand Canyon region. It is in connection with this work that the present study was made.

J.G. MacDonald (1967) studied the vertical variation in a single section from a Lower Carboniferous basalt flow in Scotland, but the abundance of secondary minerals as alteration products make any inferences on primary chemical variability suspect. Watkins, *et al.* (1967), Watkins and Haggerty (1967), Gunn, *et al.* (1968), and Watkins and Gunn (1969) have reported considerable vertical variation in the major elements, Th, U, and Fe-Ti oxides in vertical sections from Icelandic tholeiite flows. Taylor (1966) has found considerable lateral variation in major elements in 12 samples from a recent basaltic andesite flow in the Cascade Range of Oregon. These studies represent the only available data on variation in a single basaltic lava flow, and no study

EXPLANATION OF PLATE 2

EXPOSURE OF THE GUNLOCK FLOW

Panoramic view of the Gunlock flow looking north from sample section 6.

involving combined vertical and lateral sampling of a single flow has been reported.

Acknowledgments

The writer would like to express appreciation to many individuals who aided in this study, particularly Dr. Myron G. Best for his advice and continual interest in this study, Dr. Willis H. Brimhall for his advice on chemical techniques, Dr. Harold J. Bissell for his suggestions and review of the manuscript, and Dr. W. Revell Phillips for his assistance in the determination of the oxide mineralogy. In addition, the writer wishes to thank Samuel Smith, George Wilson, and Phyllis Embree for their assistance in sampling the flow. Lastly, special thanks is due my wife, Carolyn, for her typing, proofreading, and constant support and encouragement.

This study has been supported by NSF grant GA-746 to M.G. Best, W.H. Brimhall, and W.K. Hamblin.

FIELD RELATIONS

Plate 1 shows the distribution of basalt flows in the Gunlock area. These flows are of Quaternary age (Hamblin, 1963) and rest unconformably upon Mesozoic sediments (Cook, 1960). There are three distinct lithologic types of basalt in this area: the Grand Wash type represented in the Gunlock flow, the Middleton type, and the Veyo type (Best, *et al.,* 1969). The subophitic to diktytaxitic texture of the Gunlock basalt as well as the presence of dikes and pipes within the flow show its affinity to the Hurricane subtype of the Grand Wash basalt (Best, *et al.,* 1969). However, the composition and fine grain size of the basalt and the relative sparcity of the dikes indicates its transitional nature.

Gunlock Fault

The Gunlock fault displaces the Gunlock flow near sample section 3 and the Gunlock and Middleton flows east of the town of Gunlock. The fault zone strikes approximately N 10-20°E, with dips ranging from 77°E to 76°W, with westerly dips predominating. According to Dobbin (1939, p. 135) the maximum total stratigraphic separation along the Gunlock fault is approximately 4,000 feet just north of Gunlock. Where it cuts the flows, the fault shows an apparent post-basalt displacement of approximately 20 feet down to the west.

The Gunlock fault apparently dies out to the south and is replaced by the Shebit fault and Shebit anticline; the Shebit fault in turn passes into the Cedar Pocket Canyon fault farther to the south (Cook, 1960, p. 65). According to Hamblin (personal communication, 1969) these three faults represent the northernmost extension of the Grand Wash fault system.

Gunlock Flow

The oldest flow in the area is the stage IIc (Hamblin, 1963) Gunlock flow (Plate 1), exposed as an inverted valley (Hamblin, 1963) for a distance of 7.5 miles south of the community of Gunlock. It also lies in an ancient stream channel concealed beneath Veyo basalt flows at the northern edge of the area (Text-fig. 2, Section A-A'). These exposures apparently delineate an ancestral channel of the Santa Clara River, down which the Gunlock basalt flowed. This

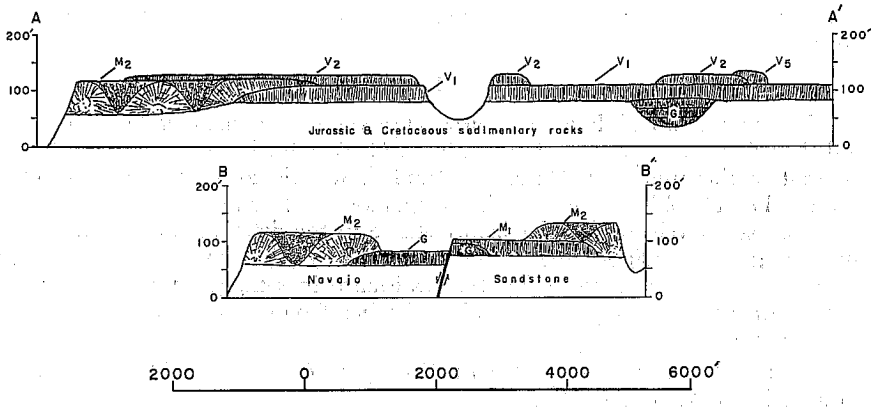

TEXT-FIGURE 2.—Stylized cross sections drawn along A-A' and B-B' in Plate 1.

conclusion is also supported by the unconsolidated stream sands and coarse gravels upon which the flow rests. In general, evidence of baking at the basalt contact is lacking, or if present, consists only of a slight bleaching due to reduction of the Fe-oxide present in the red sands.

In the field, basalt of the Gunlock flow is easily recognized by its abundant olivine phenocrysts and the conspicuous absence of quartz or plagioclase xenocrysts which characterize the Middleton and Veyo basalts.

For essentially the entire length of exposure the Gunlock flow consists of a single flow unit ranging in thickness from 25 to 30 feet in the center to approximately three feet at the edges. However, in an area extending approximately one mile north from sample section 6 there are exposed in the canyon walls two, and in one place three, distinct layers of basalt delineated by vesicular tops and rough spinose bases which conform closely to Nichols' (1936, p. 620-621) definition of multiple flow units. The irregular and rugged contacts between these units show no evidence of weathering, erosion, deposition, or soil development. The flow units are small and discontinuous with thicknesses ranging from 5 to 20 feet and widths ranging from 20 to 400 feet. None of these units are more than a mile in length as they are seen only in the two canyons one-half mile and three-quarters of a mile north of sample section 6.

These multiple flow units apparently formed as a sequence of tongues of lava advancing from, and eventually overridden by, the main flow. Thus, they are not to be considered as individual flows, but as part of one flow, and they probably all formed within a matter of hours or at most a day or two (Nichols, 1936, p. 625). Such was assumed to be the case in order to include sample section 7 with the other 6 in the study of lateral chemical variations.

In general, the base of the Gunlock flow is rough and spinose with a thin vesicular zone one and two feet in thickness. A layer of reddened clinker commonly found at the base of aa flows is generally lacking, but locally reddened, rubbly masses up to approximately 15 feet wide may be seen extending up into the flow for a few feet and even to the surface in some places.

Above the basal vesicular zone the flow is usually massive with crude columnar joints, probably corresponding to what Spry (1961, p. 197) calls

mega-columns. These mega-columns are generally on the order of four to six feet in diameter and extend from the basal layer to, or through, the three- to ten-foot thick vesicular layer at the top of the flow. Generally, vesicles start to appear slightly above the middle of the flow, but are only numerous enough to make the rock truly scoriaceous in the uppermost 2 or 3 feet. Locally, mega-columns extending downward from the top and upward from the base are separated by a zone of closely spaced (approximately one to four inches) horizontal joints. Joints of this type also appear within the thinner flow units. This zone of horizontal joints is generally one to two feet thick.

At the northern edge of the mapped area northwest of the Veyo cinder cone, a stream valley containing three flows of the Grand Wash type of basalt is concealed beneath the two oldest Veyo flows. This valley and its three flows are approximately 1,000 feet wide with the flows ranging in thickness from approximately 25 feet for the lowest, to approximately 15 feet for the upper two. All flows have typical vesicular tops and bottoms, but the break between the bottom and middle flows is more conspicuous than the contact between the middle and upper flows. It is marked by a wider gap (a foot or two) which contains some silt and fine sand and basalt clinkers. The contact between the second and third flows resembles those between flow units farther south. This fact, along with the chemical compositions of these flows (Appendix B-I) suggests that the lower flow is probably the Gunlock flow whereas the other two are flow units from a later eruption of similar material from the same source.

In many exposures the upper half of the Gunlock flow contains abundant, sharply defined pipes and dikes four inches or less across (Plate 3), plus seemingly isolated pods. These bodies are quite distinctive due to their high vesicularity, coarser texture, and sparcity of olivine phenocrysts. Similar, but better developed bodies occur in a thicker diabase flow of Hurricane type north of Cane Springs, about 40 miles to the south in northwest Arizona (Best, *et al.,* 1969, p. 15). Still other occurrences of similar bodies, generally interpreted as late residual differentiates of flows, are found in the Columbia River Plateau and in the Modoc Plateau of northern California (see Kuno, 1965).

Since the Gunlock flow is concealed beneath younger basalts to the north, its source area has not been determined. However, as it apparently follows a course ancestral to the present course of the Santa Clara River, and since at its most northerly exposure its course runs generally to the south-southwest, it is assumed that the source of this flow is in the direction of the Pine Valley Mountains to the north-northeast.

Middleton Flows

Just southeast of the town of Gunlock, the Gunlock flow is overlain by two younger stage IIc flows of the Middleton type (Best, *et al.,* 1969). This basalt type is comprised of xenocrystic labradorite-andesine laths with smaller olivine and clinopyroxene phenocrysts in an intergranular groundmass of andesine, clinopyroxene, olivine, and oxides. Xenocrysts of quartz are typical.

The oldest of the two Middleton-type flows (M_1, Plate 1) has been buried by the second (M_2) and is exposed only in two places, about one mile southeast of Gunlock and on the east side of the Gunlock fault, and about the same distance northeast of Gunlock. In the northern outcrop, M_1 rests directly on the

1

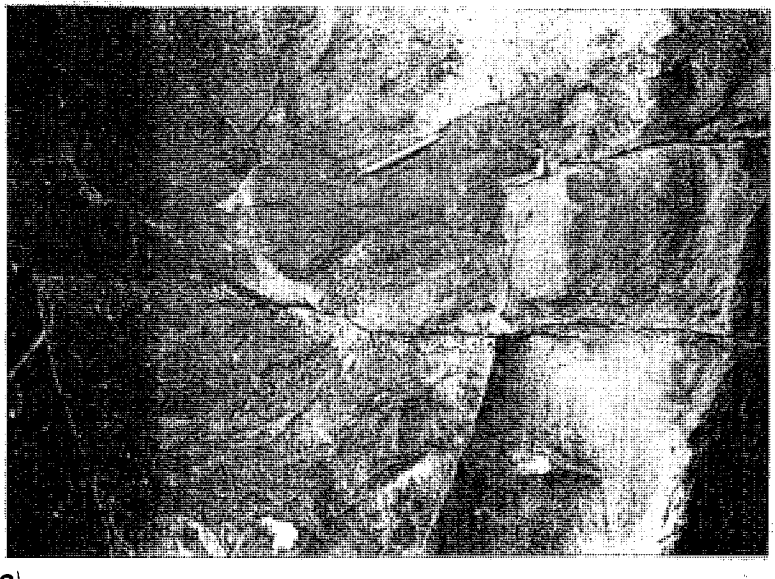

2

EXPLANATION OF PLATE 3

DIKES AND PIPES

FIG. 1.—Vesicular pipes in Gunlock basalt.
FIG. 2.—Cross-cutting vesicular dikes in the Gunlock flow.

underlying sedimentary rocks whereas to the south its western half is underlain by the Gunlock flow (Text-fig. 2, Section B-B').

M_1 is approximately 25 feet thick, crudely jointed, and superficially resembles the Gunlock flow. M_2 by contrast, is easily distinguished from the Gunlock flow, even at great distances, due to its greater thickness (approximately 60 feet), and its characteristic "sun-burst" jointing pattern. Where M_2 has been dissected by streams, it appears as a series of large (75 to 150 feet wide and 60 feet high) arch shaped bodies of radially and concentrically jointed basalt with the joint blocks produced by this pattern being 10 to 20 feet in diameter. The U-shaped areas between these "sun-bursts" are occupied by highly jointed basalt consisting of blocks approximately three feet in diameter. These joint blocks are commonly more vesicular than the massive material on either side. In some cases, a rubble or clinker zone up to 15 feet thick is found at the base of the highly jointed areas, but this is by no means universal. "Sun-bursts" probably result from water flowing down into widely spaced master joints formed early in the cooling history of the flow. This would fracture the rock around the joint, producing the U-shaped, highly jointed area and change the pattern of the isotherms from horizontal to arch-shaped between two master joints thus modifying the joint pattern. There are two possible sources for this water; 1) torrential rains accompanying volcanism; and 2) water flooding the surface of the flow as the river topped the lava dam formed by the flow where it entered the stream channel. The latter possibility seems most likely.

Not all jointing in M_2 is of the "sun-burst" type. In its northernmost mapped exposure and on the north side of the Santa Clara River, this flow ranges in thickness from 0 to 100 feet with crude jointing toward the edge but with perfectly developed 75-foot columns running from just above the base to within approximately 25 feet of the upper surface in the thickest portions. The upper quarter of the flow shows crude jointing only. It is presumed that in this area the excessive thickness and well developed jointing are due to ponding and slow cooling in a dry environment.

Veyo Flows

The Veyo basalt contains large xenocrysts of quartz similar to those in the Middleton flows, large anhedral to subhedral plagioclase phenocrysts with honeycombed glass inclusions, and in some cases, a few olivine and clinopyroxene phenocrysts in a glass-rich groundmass containing minute grains of plagioclase, clinopyroxene, hypersthene, and oxide minerals. Clinopyroxene and hypersthene with olivine are also present as microphenocrysts. This basalt type is distinctive in the respect that it is the only one in the region containing modal hypersthene (Best, *et al.*, 1969, p. 25). In the field it is recognized by its black, glassy nature, presence of large easily identifiable quartz and plagioclase grains, and the lack of the smaller abundant plagioclase laths of the Middleton flows.

At least five distinct Veyo flows have been recognized. The oldest Veyo flow (there may actually be more than one, but the field relations are obscure) is stage IIc and for the most part is concealed beneath younger flows (Plate 1). V_1 varies in thickness from 40 to 60 feet with joint pattern variations from crude widely spaced and poorly developed master joints to perfectly developed columns 2 to 3 feet in diameter, in some places showing a well developed upper and lower colonnade separated by a thin entablature (Spry, 1961, p. 194). Like

the other four Veyo flows, the upper three to ten feet of this flow are usually quite vesicular and glassy and lack well developed jointing.

The interval between V_1 and the highest Gunlock flow in the stream channel northwest of the Veyo cone is represented by three to four feet of basalt rubble and quartz sand. Elsewhere, this flow rests on sandstones of the Jurassic Navajo and Entrada formations to the south and Cretaceous sediments to the north (Cook, 1960, p. 58). The V_2 flow overlies V_1, and its eastern portion is covered by a later flow, V_3. V_2 and V_3 together, cover an extensive area south and east of the Veyo cone, and for the most part only their glassy-vesicular crust (partially concealed by soil) is exposed; these two flows have been classified as stage IV.

The youngest flows are two relatively small ones, V_4 and V_5, which emerge from the east and northwest flanks of the Veyo cone approximately one third the way up from the base. V_4 has been analyzed and described (Best, *et al.*, 1969). The relative ages of V_4 and V_5 with respect to one another cannot be determined exactly, but their relation to the cone and other flows, along with their freshness indicate that they represent the last flow activity, and may have been essentially contemporaneous with one another.

The source of all five Veyo flows is apparently the feeder for the Veyo cone, although the cone itself may not have been present at the time the earlier flows were emitted.

Pyroclastic and Alluvial Deposits

The Veyo cone (V_p Plate 1) is an unusually symmetric cinder cone approximately 500 feet high, with a base diameter of approximately 3,800 feet. It has been breached on the east side, but this may be an eruptive feature and not due to erosion as there is no corresponding alluvial deposit at the base of the breach. However, pyroclastic material from the southwest side of the cone has been deposited on bordering flows by slope wash (V_{al}, Plate 1).

The cone is composed of stratified red and black pyroclastic material ranging in size from cinder and lapilli up to blocks and bombs three feet in diameter. This material is cemented just below the surface by a layer of caliche which apparently has inhibited erosion.

PETROGRAPHY

The Gunlock flow is a fine grained alkali olivine basalt with a subophitic to diktytaxitic texture. Abundant small olivine phenocrysts lie in a matrix of plagioclase laths which are partially enclosed by pyroxene. This groundmass also contains small olivines and Fe-Ti oxides along with minor amounts of apatite. Samples from the chilled lower margin contain the same olivine phenocrysts and plagioclase laths, both surrounded by black glass, rich in minute oxides and pyroxene (?) microlites. With the exception of the chilled margins, the Gunlock basalt is glass free.

Modal Analyses

The modal variation in samples from two vertical sections (3 and 6), is shown in Text-fig. 3 and Appendix A Table I. Comparison of the calculated counting errors and the observed data show that with the exception of olivine, the counting error is only a small fraction of the variation observed. In the case of olivine, the counting error is 1 percent and may in fact be greater, due to

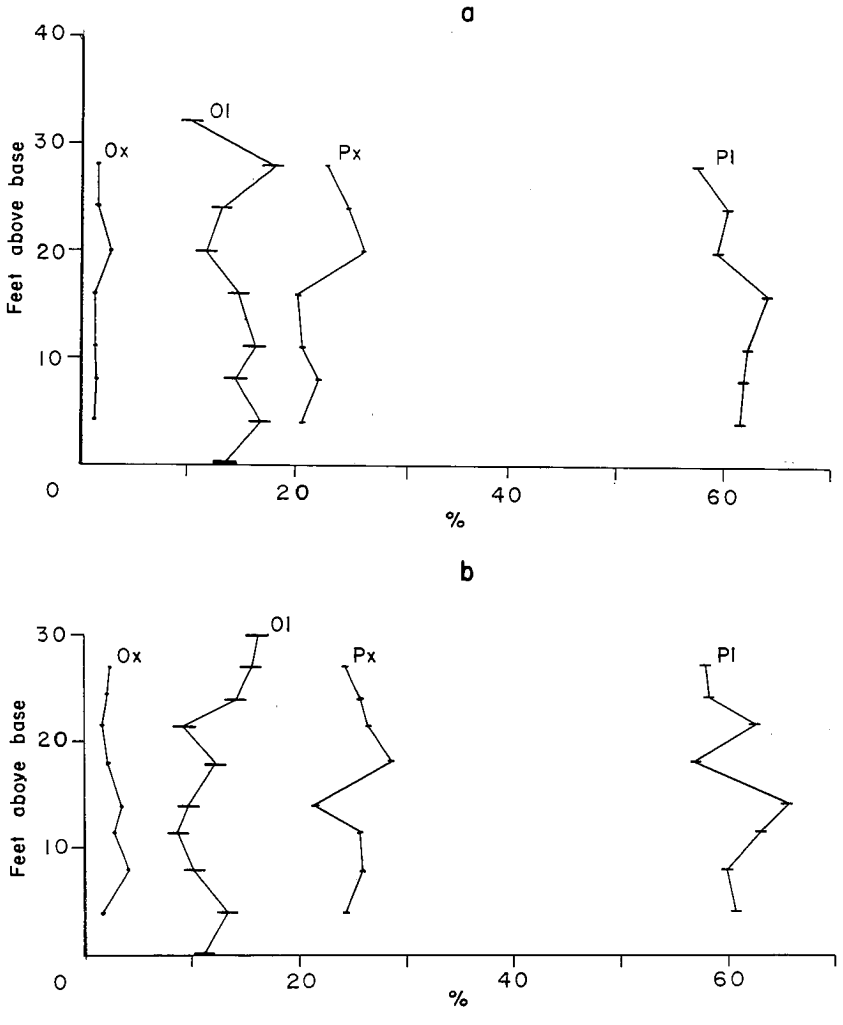

TEXT-FIGURE 3.—Modal variation in sections 3 (a) and 6 (b).

the patchy distribution of olivine phenocrysts within the rocks. However, at least half of the approximately 2.6 percent standard deviation observed for olivine is probably quite real as is the variation observed in the other minerals.

Mineralogy

Olivine.—Anhedral olivine phenocrysts (Fo_{87}; obtained from X-ray determination of d_{130}, Yoder and Sahama, 1957) up to 4 mm across plus smaller groundmass grains are found in all samples. Some vertical and lateral variation exists in the modal percentage of olivine in and between sample sections 3 and 6. The vertical variation observed in these two sections is not consistent, and the

only definable trend is an apparent weak increase in olivine from the base to the top of section 6. As this is not observed in section 3 also, it may not be a real or significant trend.

The difference of 2.3 percent in the mean modal percent of olivine between section 3 and section 6 may be a significant lateral variation; however, the data from two sections is not sufficient to define any trends in the lateral variation in olivine or other phases, and it is essential that more work be done to define such trends if they exist.

Pyroxene.—All thin sections, with the exception of those from the base of the flow, show subophitic, pale purplish brown augite grains ($En_{40}Wo_{39}Fs_{21}$) up to 1.5 mm in diameter enclosing plagioclase laths. Samples from the base of the flow show small poorly developed interstitial grains of clinopyroxene among the better developed plagioclase laths.

The modal variation in pyroxene seems to be quite comparable in sections 3 and 6 in that they both have a maximum overlying a minimum near the center. On the other hand, section 3 shows a slight tendency to increase toward the top whereas section 6 reflects a slight tendency to increase towards the center of the flow. In contrast to these trends, J.G. MacDonald (1967) demonstrates an unequivocal increase in pyroxene all the way to the top of a Scottish flow.

Plagioclase.—Small (0.5 to 1 mm) normally zoned plagioclase laths are the major constituent in all samples of the Gunlock basalt. A few thin sections contain one or two plagioclases up to 3 mm in length which are either anhedral and honeycombed with abundant inclusions of pyroxene and oxides or subhedral, calcic, with broad oscillatory zoning. These grains make up less than 0.1 percent of the rock and are extremely spotty in distribution.

There is an apparent overall decrease in the concentration of plagioclase from the base to the top of the flow. The ranges in the An-contents of the plagioclase grains in section 6 are plotted opposite their relative positions in Text-fig. 4. The variation in this section is by no means consistent. The only apparent trend is a general increase in minimum An-content toward the top. However, the top and bottom samples do not conform to this trend.

J.G. MacDonald (1967) has found similar modal variations in a Scottish lava flow. He reports a decrease in the content of feldspars toward the upper part of the flow, a corresponding increase in olivine and augite, and an irregular variation in the concentration of Fe-Ti oxides. A corresponding upward increase in the anorthite content of the plagioclase was also reported. Although the overall variation in plagioclase composition in section 6 of the Gunlock flow is irregular, the upward increase in the minimum anorthite percent reflects, to some extent, the observations of MacDonald.

Fe-Ti Oxides.—Primary subhedral to anhedral oxide grains (up to approximately $\frac{1}{3}$ mm across) are evenly distributed throughout the groundmass of the basalt. Secondary oxidation of olivines and pyroxenes has, in many samples, produced patches of oxides in and around the margins of these minerals. Minute euhedral grains of primary oxides are also found as inclusions in some of the olivine phenocrysts. These inclusions are usually small in number and are randomly located in the outer portions of the phenocrysts.

The oxide phases show no consistent variation in modal concentration within these two sample sections. However, section 6 apparently has a slightly higher

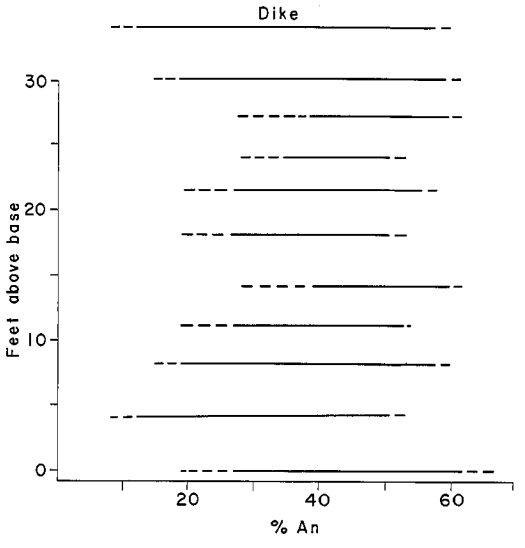

TEXT-FIGURE 4.—Range in An content of plagioclase in section 6 and in a sample of the dike basalt. Determinations were made from the index of refraction for α with the use of Figure 18 of Deer, Howie, and Zussman (1966, p. 327).

overall oxide content and shows more variation than does section 3. In spite of this lack of consistent modal variation, oxides do show textural and mineralogical variation. This variation is a critical indicator of oxidation and temperature conditions during crystallization and cooling and will be discussed in greater detail in another section.

Apatite.—Minute needles of apatite make up less than 1 percent of the rock.

Dikes

Basalt forming the dikes, pipes, and isolated pods has an intergranular texture with a modal composition distinctly different from the surrounding basalt (Table A-1 in the Appendix and Plates 4 and 5). In the Gunlock dikes the plagioclase laths are larger than those of the host basalt (up to approximately 2 mm long), and are more sodic (Text-fig. 4). The interstitial, rarely subophitic pyroxenes are smaller than the plagioclase laths (approximately 1 mm long), and are more Fe rich ($En_{24}Wo_{36}Fs_{40}$). Proportions of plagioclase and pyroxene in the dike are essentially the same as those in the host basalt. Olivine phenocrysts are, however, sparce, and groundmass olivines are absent. The content of oxide minerals in the dikes is four to seven times as great as it is in the basalt, and acicular apatites make up a substantial percentage of the rock. In the flow at Cane Springs (see Best, *et al.*, 1969, p. 15) the mineralogy and texture of the dikes are essentially the same as in the Gunlock dikes, but the host rock is much coarser grained than the dike rock (compare Plates 4 and 5).

The scarcity of olivine, the relatively low minimum An-content of the plagioclase, the more Fe-rich pyroxenes, and the abundance of apatite and oxide

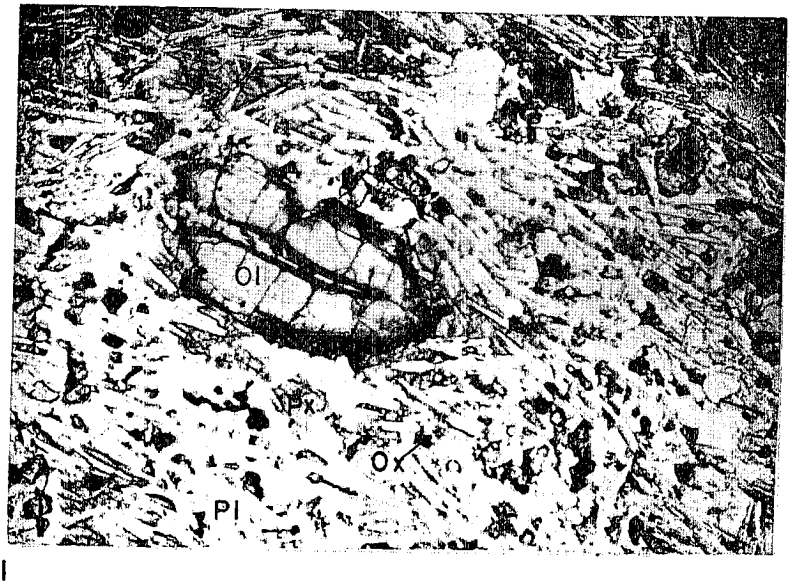

1

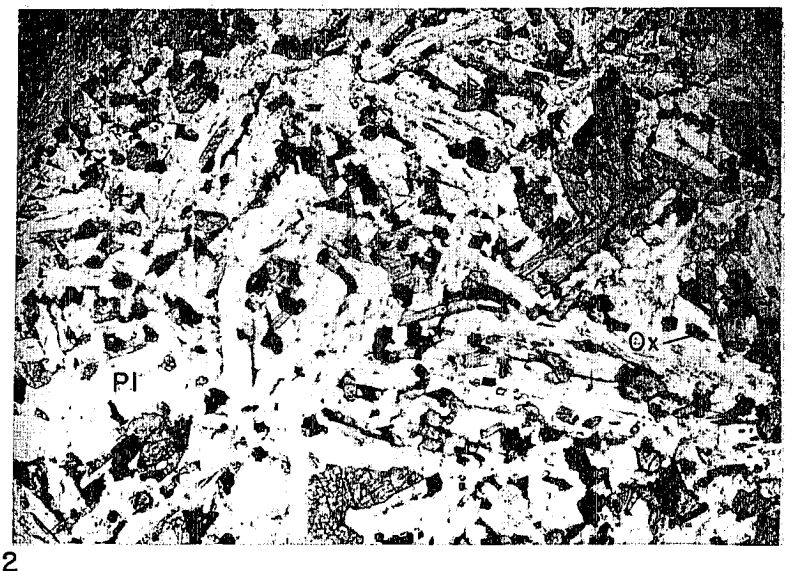

2

EXPLANATION OF PLATE 4

PHOTOMICROGRAPHS OF THE GUNLOCK HOST AND DIKE ROCKS

FIG. 1.—Gunlock host basalt. Magnification 32X.
FIG. 2.—Dike basalt from the Gunlock flow. Magnification 32X.

1

2

EXPLANATION OF PLATE 5

PHOTOMICROGRAPHS OF THE CANE SPRINGS HOST AND DIKE ROCKS

FIG. 1.—Host rock from the flow of Hurricane diabase near Cane Springs, Arizona. Magnification 32X.

FIG. 2.—Dike rock from the flow of Hurricane diabase near Cane Springs, Arizona. Magnification 32X.

minerals as well as the high vesicularity of these dikes indicate that they formed from crystallization of a late volatile-rich residual liquid from the Gunlock melt.

OXIDE MINERALOGY

The importance of Fe-Ti oxides as guides to the petrogenesis of basalts has been pointed out by Buddington and Lindsley (1964) who have shown the value of co-existing cubic- and rhombohedral-oxide phases as geothermometers and oxygen barometers. Watkins and Haggerty (1967) have demonstrated considerable variation in the degree of oxidation of these minerals in vertical sections through several individual Icelandic basalt flows; this variation has a great effect on the intensity of magnetization, and the degree of oxidation of the whole rock possibly has an effect on the Th and U concentrations. They have thus suggested a possible problem in representative sampling of basalts for radioactive and magnetic studies.

Terminology for the various Fe-Ti oxides in the literature is not entirely consistent. In the following discussion, the term cubic grains will refer to grains which initially crystallized as isometric magnetite-ulvöspinel solid solutions, and rhombohedral grains will refer to those which crystallized as rhombohedral hematite-ilmenite solid solutions. Subsequent oxidation of these grains produces complex intergrowth textures and compositional assemblages so that, for example, rhombohedral hematite might occur as an intergrowth in a cubic grain.

A study of the oxide minerals from section 6 in the Gunlock flow was done by X-ray diffraction and polished section examination under oil at 800X magnification. In the treatment which follows, use will be made of the oxidation index (OI in Table I) of Watkins and Haggerty (1967, p. 258). In brief, the

TABLE I
Oxide Mineralogy

	Cubic								Rhomb.					
Sample	mt	tm	th	mi	ru	pb	sp	γ	th	ru	pb	OI	Usp Content	Rock FeO/Fe_2O_3
6-30		+	+					—	—		+	II	Moderate	2.82
6-27		+	+					—	+		+	II	Moderate	
6-24	+		+	—	+				+	—	+	IV	Nil	
6-21.5	+		x	—	x				+	—	+	IV	Nil	1.58
6-18	+		+	—	+	+	—		+	—	+	VI	Nil	
6-14	+		+	—	—	+	—		+	—	+	V	Nil	0.84
6-11.5	+		+	—	+				+		+	IV	Nil	
6-8	+		+	—	+	+	—		+		+	VI	Nil	0.90
6-4	+		+	—	+	+	—		+	—	+	V	Nil	1.57
6-0		+	+		—	+			+		+	VI	High	1.45

Mineral phases identified optically and by X-ray diffraction (+), by optical methods alone (—), and by X-ray diffraction alone (x) in the cubic and rhombohedral grains of each sample. The oxidation index (OI), the relative amount of ulvöspinel (Usp) in magnetite (determined from lattice parameters given by Basta, 1960, p. 1,038), and the whole rock FeO/Fe_2O_3 weight ratios (derived from Fe_2O_3 determinations by A. G. Loomis) are also given. mt=magnetite; m=titanomagnetite; th=titanohematite; mi="metailmenite"; ru=rutile; pb=pseudobrookite; sp=Mg-Al(?) spinel; and γ=titanomaghemite.

ascending scale of indices is defined by the presence of the following mineral phases in the cubic grains:

I. Homogeneous titanomagnetite.
II. Titanomagnetite containing a small number of ilmenite lamellae.
III. Titanomagnetite with abundant lamellae of ilmenite.
IV. Ilmenite lamellae of III become mottled as a result of the formation of lighter colored "metailmenite", a submicroscopic intergrowth of rutile and titanohematite (Wilson and Haggerty, 1966).
V. Presence of optically distinguishable rutile is diagnostic.
VI. Presence of pseudobrookite is characteristic.

Descriptions of Samples

Rhombohedral grains generally consist of an irregular intergrowth of pseudobrookite and titanohematite (Plate 6, fig. 1). However, some samples also contain less oxidized grains with sigmoidal rutile intergrowths in titanohematite.

The following mineral phases and their textures were observed in the cubic grains of samples 6-30 through 6-0:

6-30.—Most cubic grains are essentially pure titanomagnetite, although some (Plate 6, fig. 2) show low temperature oxidation of titanomagnetite to titanomaghemite.

6-27.—Cubic grains consist of titanomagnetic showing some low temperature oxidation to titanomaghemite (Plate 7, fig. 1), or of a titanomagnetite-titanomaghemite intergrowth with a few ilmenite lamellae (Plate 7, fig. 2).

6-24.—Most grains are composed of a lamellar intergrowth of magnetite and "metailmenite", similar to that in Plate 8, fig. 2, but in a few the titanohematite and rutile have become just coarse enough to be distinguishable (Plate 8, fig. 1).
6-21.5—Lamellar intergrowths of magnetite and "metailmenite" predominate (Plate 8, fig. 2).

6-18.—Most grains consist of pseudobrookite in a titanohematite-rutile intergrowth, while some retain polygonal remnants of magnetite with Mg-Al(?) spinel (Plate 9, fig. 1). Plate 9, fig. 2 shows the typical development of irregular pseudobrookite lamellae after ilmenite in a titanohematite-rutile intergrowth.

6-11.5 and 6-14.—Fine lamellar intergrowths of mottled titanomagnetite (dark gray) and "metailmenite" (light gray) are shown in Plate 10, fig. 1.
6-8.—Irregular pseudobrookite lamellae in titanohematite-rutile intergrowths predominate (Plate 10, fig. 2).

6-4.—Assemblages of oxidation index IV to VI occur, but V grains predominate. Plate 11, fig. 1 shows polygonal areas of magnetite containing Mg-Al(?) spinel (black needles) with lamellae of "metailmenite". Plate 11, figure 2 shows another grain which has been further oxidized to an intergrowth of titanohematite-rutile with pseudobrookite lamellae and remnants of magnetite containing spinel.

6-0.—Polygonal remnants of magnetite and irregular lamellae of pseudobrookite (pseudomorphic after ilmenite) are situated in a patchy titanohematite-rutile intergrowth.

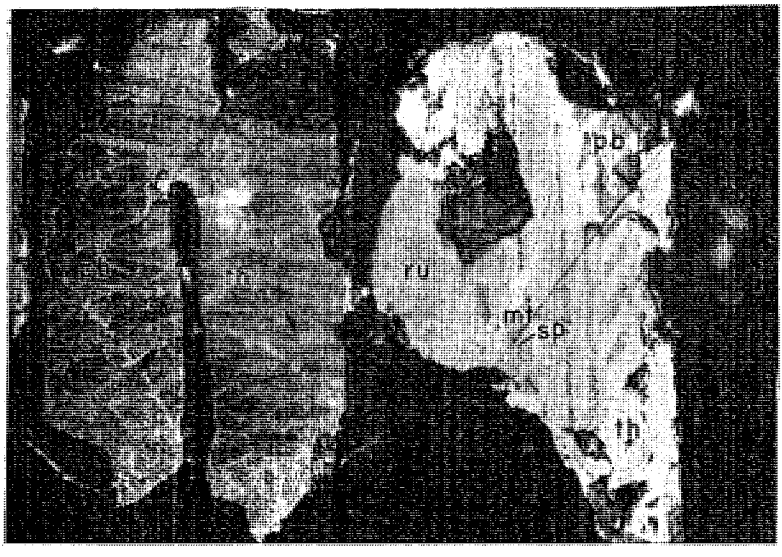

1

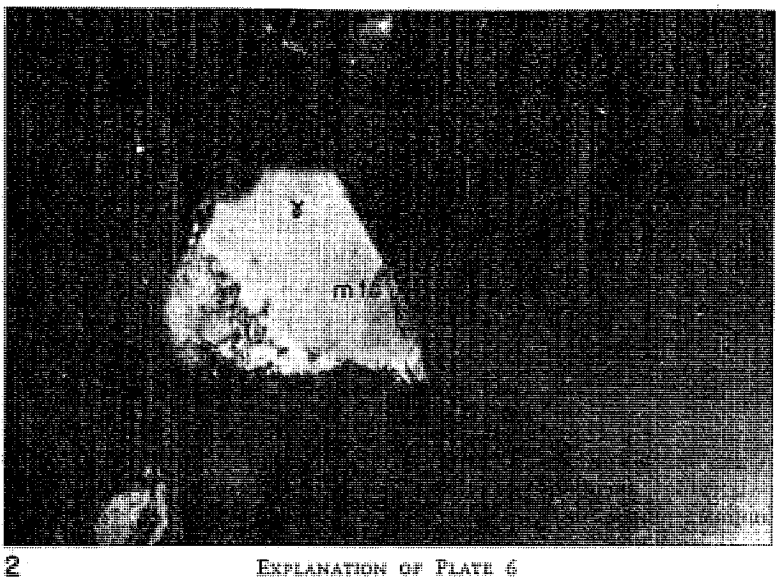

2

EXPLANATION OF PLATE 6

PHOTOMICROGRAPHS OF OXIDE GRAINS

FIG. 1.—Irregular intergrowth of pseudobrookite and titanohematite. x 650.
All figures are of oxide grains under plane-polarized reflected light in samples from section 6 of the Gunlock flow. Descriptions are in the text under "Descriptions of Samples." mt = titanomagnetite-magnetite; il = ilmenite; th = titanohematite; ru = rutite; pb = pseudo-brookite; γ = titanomaghemite; mi = "metailmenite+; sp = spinel. Magnification 650X.

FIG. 2.—Cubic grains of titanomagnetite with low temperature oxidation of titanomagnetite to titanomaghemite. Sample 6-30, x 650.

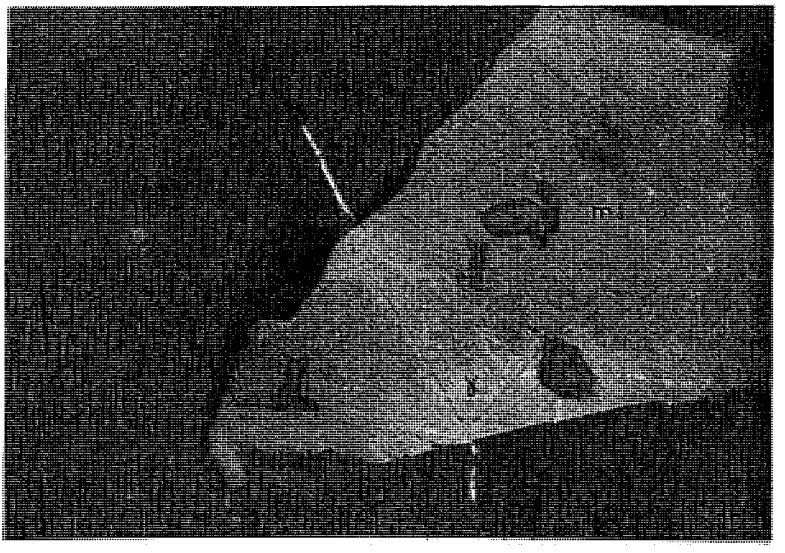

1

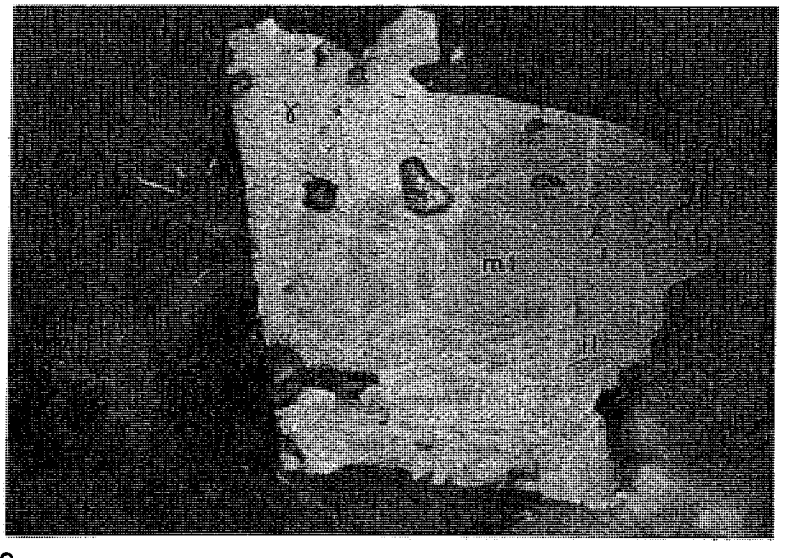

2

EXPLANATION OF PLATE 7

PHOTOMICROGRAPHS OF OXIDE GRAINS

FIG. 1.—Cubic grains of titanomagnetite with low temperature oxidation to titanomaghemite. Sample 6-27, x 650.

FIG 2.—Titanomagnetite-titanomaghemite intergrowth with a few ilmenite laminae. Sample 6-27, x 650.

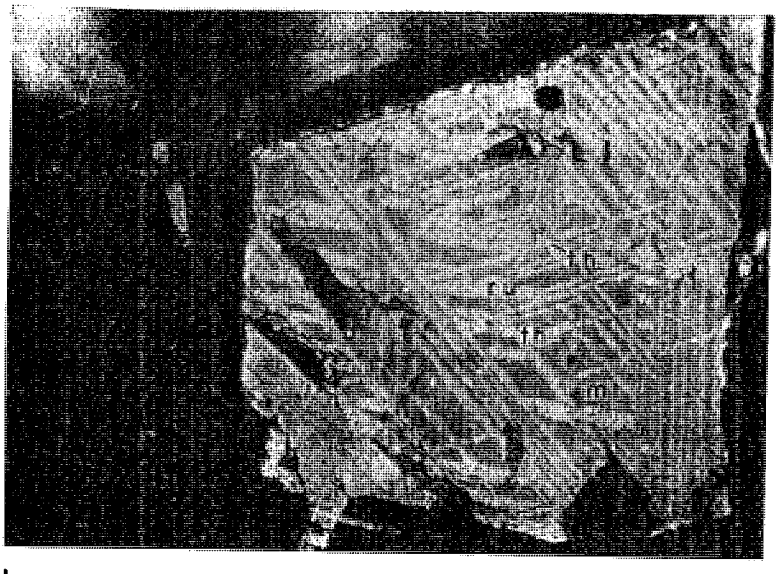

1

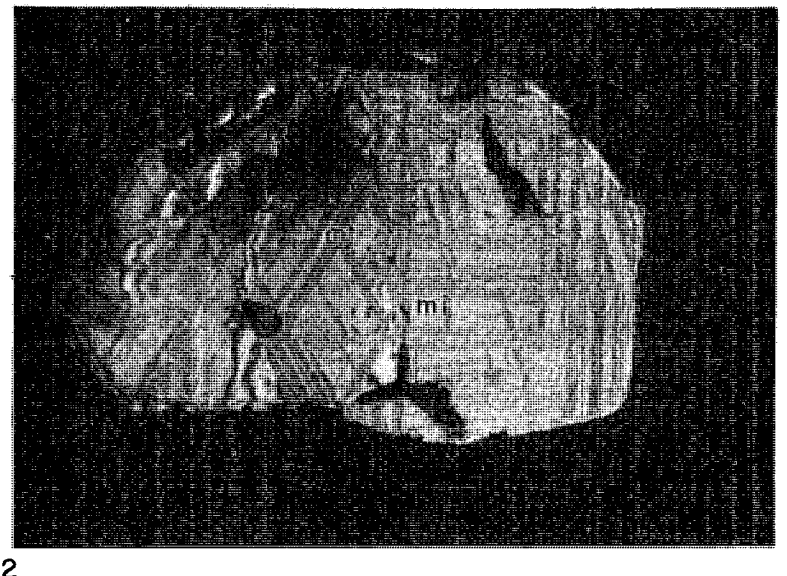

2

EXPLANATION OF PLATE 8

PHOTOMICROGRAPHS OF OXIDE GRAINS

FIG. 1.—Titanohematite and rutile grains. Sample 6-24, x 650.
FIG. 2.—Lamellar intergrowth of magnetite and "metailmenite." Sample 6-21.5, x 650.

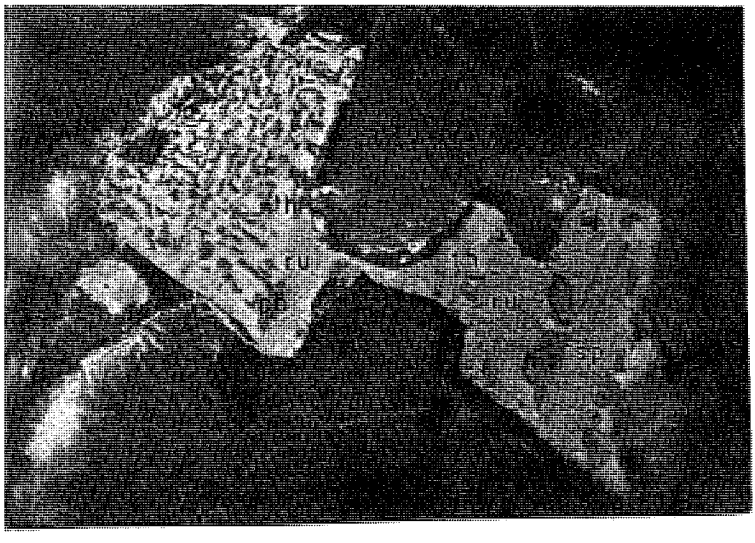

1

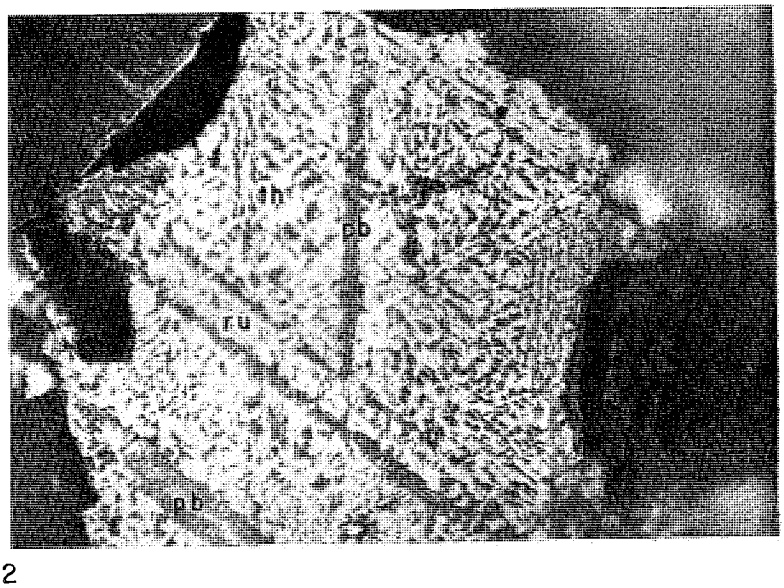

2

EXPLANATION OF PLATE 9

PHOTOMICROGRAPHS OF OXIDE GRAINS

FIG. 1.—Pseudobrookite in a titanohematite-rutile intergrowth which retains some polygonal remnants of magnetite with Mg-Al(?) spinel. Sample 6-18, x 650.

FIG. 2.—Typical irregular pseudobrookite lamellae after ilmenite in a titanohematite-rutile intergrowth. Sample 6-18, x 650.

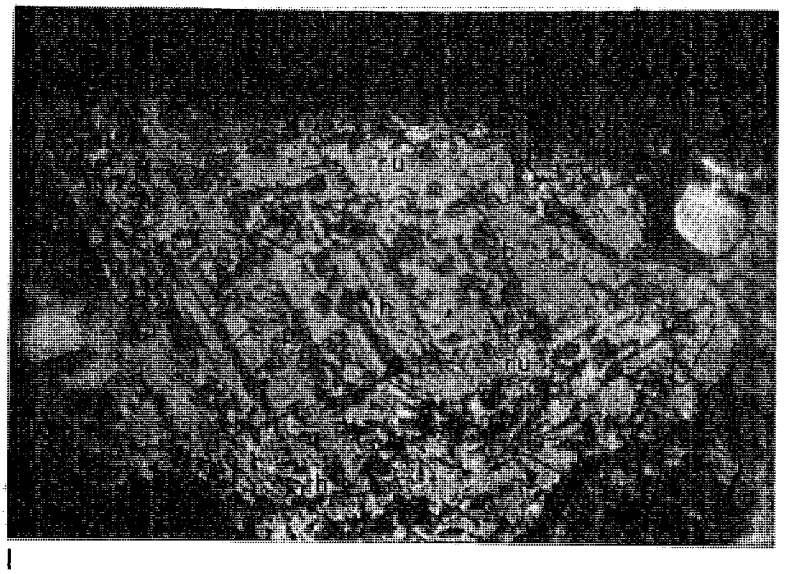

1

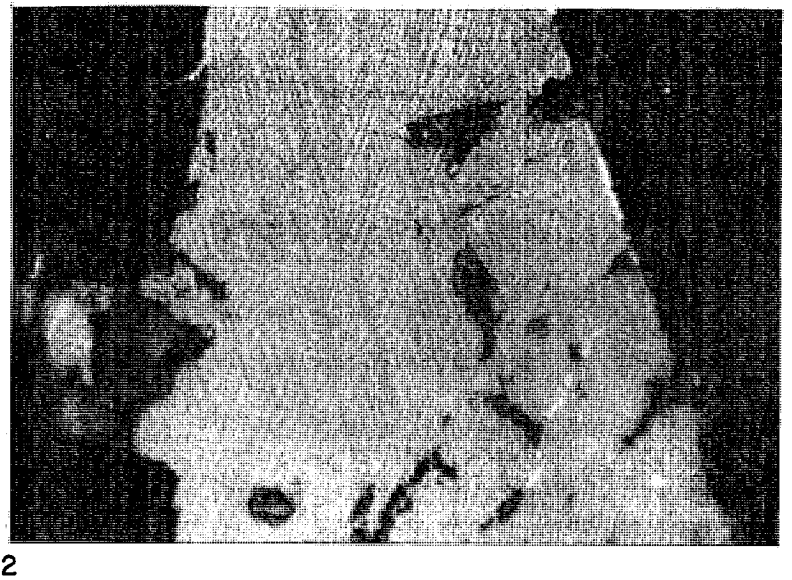

2

EXPLANATION OF PLATE 10

PHOTOMICROGRAPHS OF OXIDE GRAINS

FIG. 1.—Dark mottled titanomagnetite intergrowths with light gray "metailmenite." Sample 6-14, x 650.

FIG. 2.—Intergrowths of irregular pseudobrookite lamellae in titanohematite-rutile. Sample 6-8, x 650.

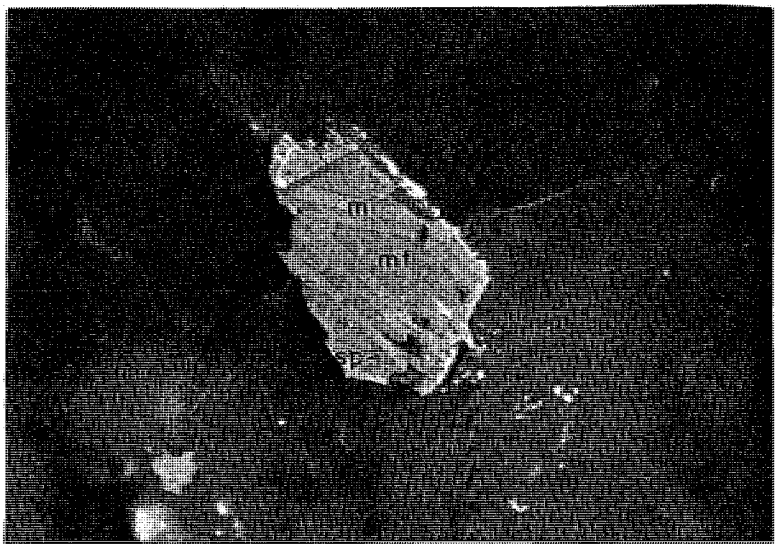

1

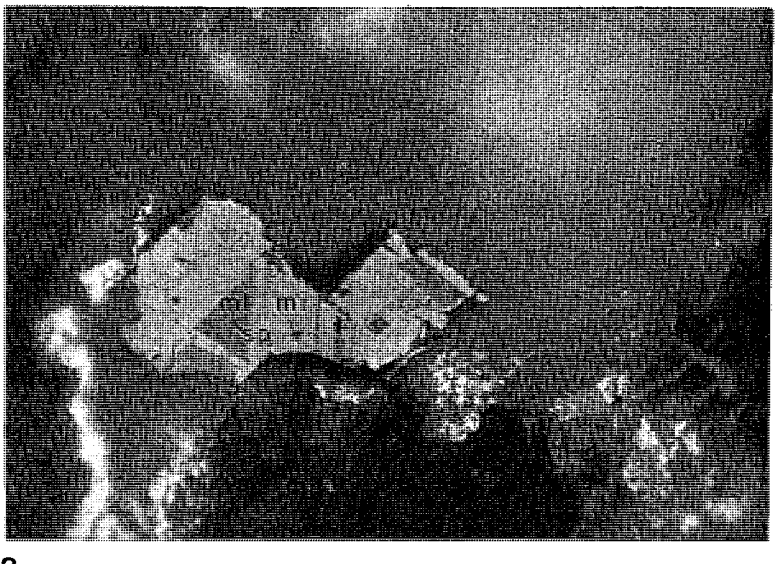

2

EXPLANATION OF PLATE 11

PHOTOMICROGRAPHS OF OXIDE GRAINS

FIG. 1.—Polygonal areas of magnetite containing black needles of Mg-Al(?) spinel with lamellae of "metailmenite." Sample 6-4, x 650.

FIG. 2.—Intergrowth of titanohematite-rutile with pseudobrookite lamellae and remnants of magnetite which contains spinel. Sample 6-4, x 650.

Textural and Modal Relations

Cubic and rhombohedral grains are present in the groundmass of the Gunlock basalt in approximately equal proportions in all samples except 6-0. Here the rhombohedral grains greatly predominate, and the grain sizes are considerably smaller than in the other samples. These facts, along with the high glass content of this sample, indicate quenching shortly after the oxides started to crystallize, with initial crystallization of the cubic grains preceeding that of the rhombohedral grains. The relatively high Ti-content of the cubic grains in this sample, inspite of its high oxidation index, indicates that early formed cubic oxides are greatly enriched in Ti. The moderately high ulvöspinel content of 6-27 and 6-30, on the other hand, is due to the low degree of oxidation at the top of the flow.

Samples 6-27 and 6-30 show what appears under the microscope to be an intergrowth of titanomagnetite and titanomaghemite (Plate 6, fig. 2 and Plate 7, figs. 1 and 2), presumably resulting from relatively low temperature oxidation of titanomagnetite (Watkins and Haggerty, 1967). This is reflected in the low oxidation index of these samples which indicates that the top of the flow did not retain a sufficiently high temperature long enough to form phases such as "metailmenite," rutile, or pseudobrookite.

Temperature-Oxidation Relations

Text-fig. 5 is a plot of oxidation index verses position of sample in the flow, and compares closely to a similar plot for an Icelandic tholeiite (Watkins and Haggerty, 1967, p. 261). The section shows maximum oxidation at the base and central parts of the flow with minimum oxidation at the top. Comparison of Text-fig. 5 with a theoretical temperature profile (Text-fig. 6) demonstrates a definite similarity between the temperature distribution and

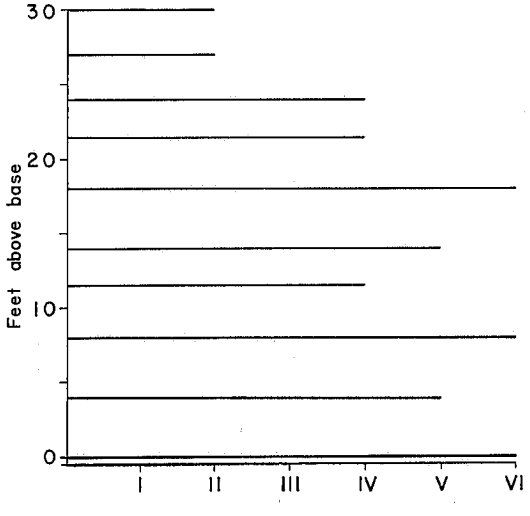

TEXT-FIGURE 5.—Oxidation index plotted against position in section 6 of the Gunlock flow. Ordinate is distance from the base of the flow in feet.

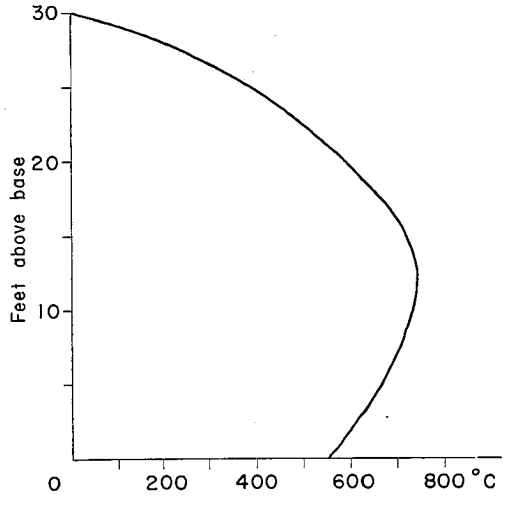

TEXT-FIGURE 6.—Theoretical temperature distribution 1.1 years after extrusion of the Gunlock flow. Calculated from curves and equations of Jaeger (1968, p. 511).

oxidation indices. Samples containing pseudobrookite, which forms at temperatures in excess of approximately 600°C (Lindsley, 1965), are found only in the parts of the flow which retain high temperatures for the longest period of time.

Sato and Wright (1966) observed oxidation phenomenon in the Makaopuhi lava lake, Hawaii, six months after its formation. They found a zone of high oxygen fugacity (10^{-6} bars) in several drill holes between 550° and 750°C (corresponding closely to the inferred temperatures of formation for pseudobrookite which migrated downward as the lake cooled. Similar zones characterized by alteration of olivines and ilmenite and by high magnetic susceptibility have been found in the Alae and Kilauea Iki lava lakes (Sato and Wright, 1966).

Sato and Wright suggest that in this temperature range (550° to 750°C) the basalt has cooled enough to restrict diffusion of O_2 and H_2O, but not H_2. With thermal decomposition of H_2O, the oxygen fugacity will thus rise substantially in this zone. Hence, rutile and pseudobrookite could easily be formed in this zone. Such a mechanism appears to adequately explain the existence of high degrees of oxidation in the central and lower part of the Gunlock flow as well as in Icelandic flows studied by Watkins and Haggerty (1967).

Since the top (Samples 6-27 and 6-30) of the Gunlock flow cooled relatively rapidly, there was not enough time for a high degree of oxidation to develop. Temperatures of 550° to 750°C and the developing high oxidation zone probably remained in the area of 6-21.5 and 6-24 for only a short time allowing the formation of rutile only. Below this part of the section the temperatures remained high long enough for even higher oxygen fugacities to develop, and pseudobrookite formed at successively lower levels as the flow cooled. The cause of irregular variation in the oxidation indices in the lower half of the flow is uncertain. However, this is evidently the normal case as both Watkins

and Haggerty (1967) and Evans and Moore (1968) have reported similar irregular variations. Evans and Moore (1968, p. 106) have suggested that the relative proximity of collected samples to joints may cause these variations. This appears to be the best explanation, as this would locally open the system to outward migration of O_2 and H_2O near the joints.

Phase Relations

Phase relations in the system FeO-Fe_2O_3-TiO_2 at 1,300°C (Taylor, 1964) do not adequately account for several of the relationships found in the Gunlock and other basaltic flows. In particular, the oxidation of titanohematite to rutile, rather than pseudobrookite, is not predicted. A stability field involving titanohematite and rutile is not present, although textural relations indicate that one must exist. Lindsley (1965) states that the pseudobrookite series decomposes to hematite, ilmenite, and rutile, as the temperature decreases from 1,140°C at the $FeTi_2O_5$ end to ~600°C at the Fe_2TiO_5 end. This breakdown would permit the formation of a two phase, rutile-titanohematite field and a three phase rutile-pseudobrookite-titanohematite field (Text-fig.7) at approximately 700°C. A diagram such as Text-fig. 7 would explain the sequence of mineralogical

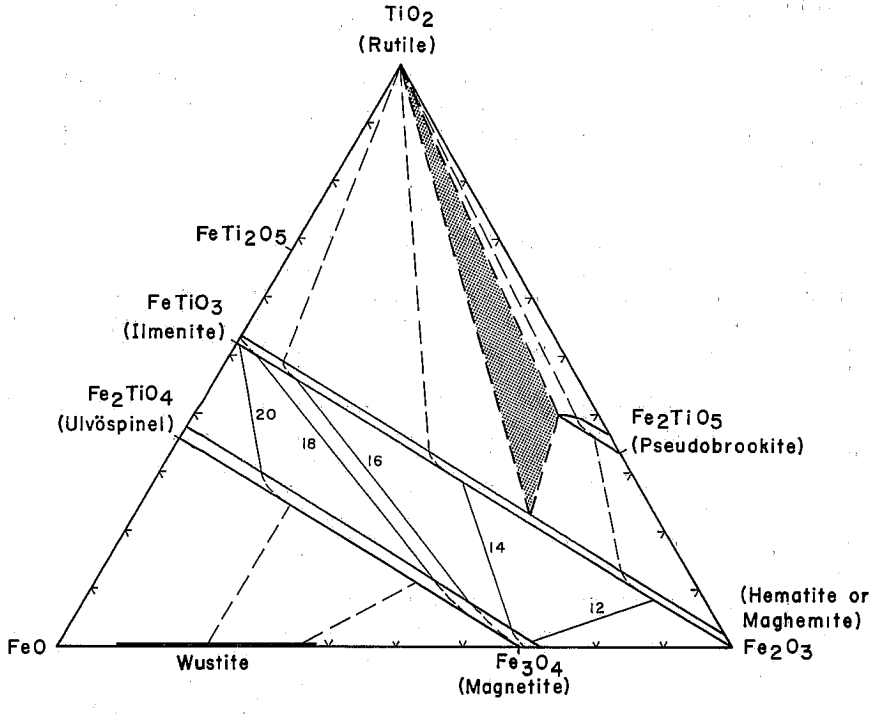

TEXT-FIGURE 7.—Hypothetical, phase relations in the system FeO-Fe_2O_3-TiO_2 at approximately 700°C. Heavy lines are field boundaries and fine lines are isobars (solid and labled in -log fO_2 where determined from data in Buddington and Lindsley, 1964). The 3 phase rutile, pseudobrookite, titanohematite field is shaded.

and textural relationships in the oxide minerals of this section in the Gunlock flow as well as those described by Watkins and Haggerty (1967).

Whole Rock Oxidation Characteristics

The variation in oxidation index observed in polished sections is not at all evident in the corresponding thin sections. Although all samples show some reddening of olivines, and in some cases pyroxenes, in thin section, there is no consistent relationship between the oxidation index and the degree of apparent reddening. Thus it is evident that polished sections as well as thin sections must be examined before the chemical composition or magnetic properties of a sample can be considered to be unaltered by oxidation (Watkins and Haggerty, 1967). On the other hand, the variation in the whole rock FeO/Fe_2O_3 ratio shown in Table I corresponds closely to the temperature curve (Text-fig. 6) and the variation in OI (Text-fig. 5). In this case, individual samples do not always show analogous variations in the OI and the FeO/Fe_2O_3 ratio, but when the overall trends are considered, the agreement is good.

GEOCHEMISTRY

Analytical Methods

Samples of approximately one kilogram were taken from the Gunlock flow in the pattern previously described. Each sample, crushed to minus 60-mesh, was homogenized, and a 500 gm sample was split from the crushed material for determination of Th, U, and K (denoted as gK_2O in the Tables) by gamma-ray spectrometry. The remainder was crushed to minus 80-mesh, and 0.2500 gm was prepared by a fusion technique described in detail by Brimhall and Embree (1969a) for determination of Si, Al, Na, K (denoted as aK_2O in the Tables), Ca, Mg, total Fe, and Ti by atomic absorption spectrometry.

The instrumental precision for the gamma-ray analyses was determined by seven replicate measurements of a single sample. The overall precision for the atomic absorption analyses was determined by preparing and analyzing nine samples from a homogenized standard designated Gunlock "Standard" made up of equal proportions of all samples from sections 1 through 6. The results of these replicate determinations are discussed by Brimhall and Embree (1969b). The precision obtained for each element, including Th, U, and gK, are represented in Table II in terms of standard deviation and relative deviation,

$$\frac{\text{standard deviation}}{\text{mean}} \times 100$$

Determinations of FeO and total Fe for some of the samples from section 6 were provided by A.G. Loomis (Table III). A comparison of my total Fe determinations with those of Loomis reveals a discrepancy of 0.04 percent and 0.08 percent respectively for samples 6-8 and 6-14. This comparison gives an indication of the accuracy, at least for total Fe, of the atomic absorption analyses.

Chemical Variations

The study of chemical variation in a flow involves two problems, 1) determination of the magnitude of variations which must be made for accurate interflow comparisons, sampling techniques, and regional classification schemes; and 2) determination and interpretation of any consistent trends in variation.

Magnitude of variation.—The chemical composition of each sample from sections 1 through 7 is shown in Appendix B, Tables II-VIII. The mean composition and variation (standard deviation) has been calculated for each section (Table B-IX). The maximum standard deviation found for each element in any one of the seven sections is shown along with the experimental precision, in Table II. A comparison of the data presented in this Table shows that, with respect to the major elements, vertical variations are at least two times, and in most cases four to seven times as great as the experimental error. Thus, the observed vertical variations are real and not a result of analytical error. Uranium has a vertical variation in excess of its experimental error, and thus, at least part of the U variation expressed must be real. Th, on the other hand, has a smaller vertical variation than instrumental error, therefore any variation in Th is below the limits of detection by this method and the Gunlock flow must be

TABLE II
Intraflow Chemical Variation and Instrumetal Precision

	Gunlock Standard			Any Section;	Entire Flow;	Any Type;
	Mean	s	r	max.s	s	min.s
SiO_2	49.20	0.24	0.49	0.56	0.27	0.59
Al_2O_3	16.20	0.05	0.31	0.27	0.10	0.69
FeO	9.98	0.04	0.40	0.18	0.08	0.46
MgO	8.53	0.06	0.70	0.44	0.18	0.55
CaO	8.48	0.12	1.42	0.42	0.18	0.43
Na_2O	3.52	0.02	0.57	0.15	0.07	0.18
aK_2O	1.04	0.01	0.96	0.06	0.04	0.14
TiO_2	1.65	0.01	0.61	0.07	0.03	0.14
Mg/Fe	0.66	0.01	1.52	0.03	0.01	——
Fe/Ti	7.83	0.06	0.77	0.33	0.13	——
	Single sample, 7 runs					
gK_2O	1.07	0.01	0.93	0.07	0.04	0.15
Th	1.76	0.21	11.93	0.17	0.05	1.00
U	0.46	0.04	8.70	0.07	0.03	0.19
Th/U	3.86	0.68	17.62	0.78	0.27	——

The mean, standard deviation (s), and relative deviation (r) for the nine replicate samples of the Gunlock Standard and for the seven runs of a single gamma-ray sample are given as a check on instrument precision. These are compared to the maximum standard deviation found for each constituent in any of the seven vertical sections, the standard deviation found for the mean of all 7 sections, and the minimum standard deviation for any constituent in any of the regional basalt types given in Table 2 of Best, *et al.*, 1969. Oxides are given in percent, while Th and U are in ppm. Total iron is given as FeO, aK_2O is K_2O determined by atomic absorption, and gK_2O is K_2O by gamma-ray spectrometry.

TABLE III
Comparative Fe determinations in weight %

Sample	6-0	6-4	6-8	6-14	6-21.5	6-30
Total Fe as FeO						
(Loomis)	——	——	10.06	9.92	——	——
(Embree)	10.12	10.12	10.10	9.84	10.06	10.06
FeO (Loomis)	6.24	6.43	5.04	4.76	6.40	7.63
Fe_2O_3 (by difference)	4.31	4.10	5.62	5.64	4.06	2.70

considered to have essentially a uniform Th content. Since the Th/U ratio is dependent upon the Th content, variation in this ratio within the Gunlock flow must also be considered insignificant.

The lateral variation in the chemical composition of the Gunlock flow was determined by calculating the mean and standard deviation for the seven vertical sections. These standard deviations are listed in Table II, and when compared with the maximum vertical variation in each constituent for any section (Table II) they show that there is considerably less lateral variation than vertical variation.

Trends in variation.—As can be seen in Tables B-II through B-VIII in the Appendix, the vertical variation in concentrations of any of the analyzed constituents is by no means entirely consistent in all sections. However, for some constituents, several, though not all, sections show similar trends. To obtain a general picture of vertical variations, the data for each constituent from all seven sections have been combined into a single plot where thickness of the flow has been normalized to 30 feet. The following discussion is based primarily on these plots, Text-figs. 8 through 12.

SiO_2 and Al_2O_3.—In most individual sections, as well as in the composite section (Text-fig. 8a), SiO_2 shows a marked decreased in the upper part of the flow. There may also be a slight decrease at the base but more data is needed to substantiate this possibility. The basal chill appears, on the basis of two samples, to be richer in SiO_2 than the upper chill.

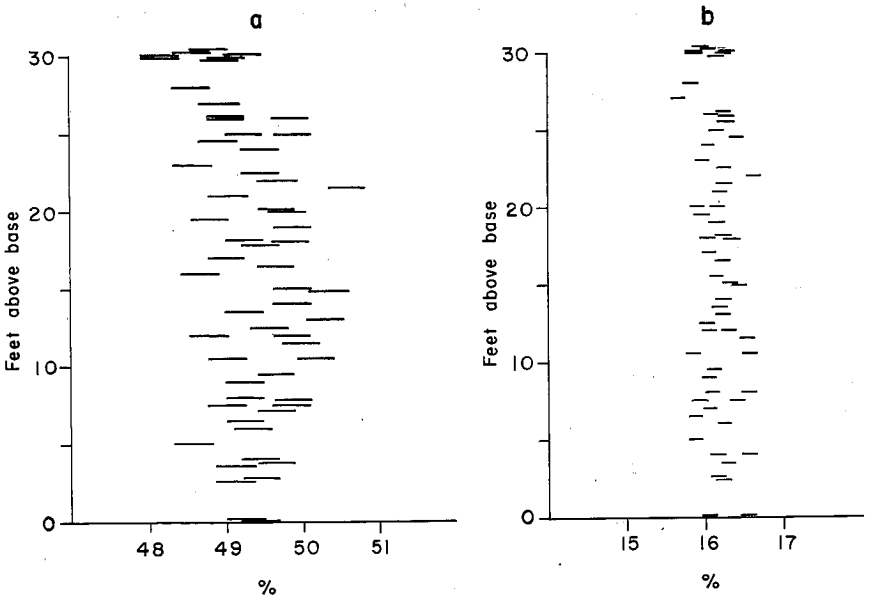

TEXT-FIGURE 8.—Composite plots for SiO_2 (a) and Al_2O_3 (b). All seven vertical sections were normalized to a thickness of 30 feet. Length of horizontal bars indicates instrumental precision (as standard deviation). Lines were staggered at 30 feet to avoid crowding. These specifications are the same for Text-figures 8 through 12.

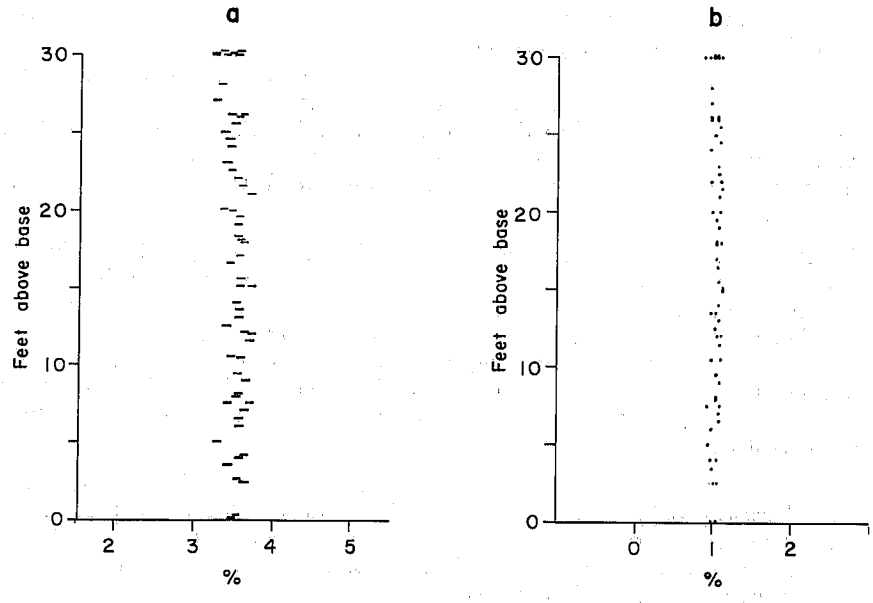

TEXT-FIGURE 9.—Composite plots for Na_2O (a) and aK_2O (b).

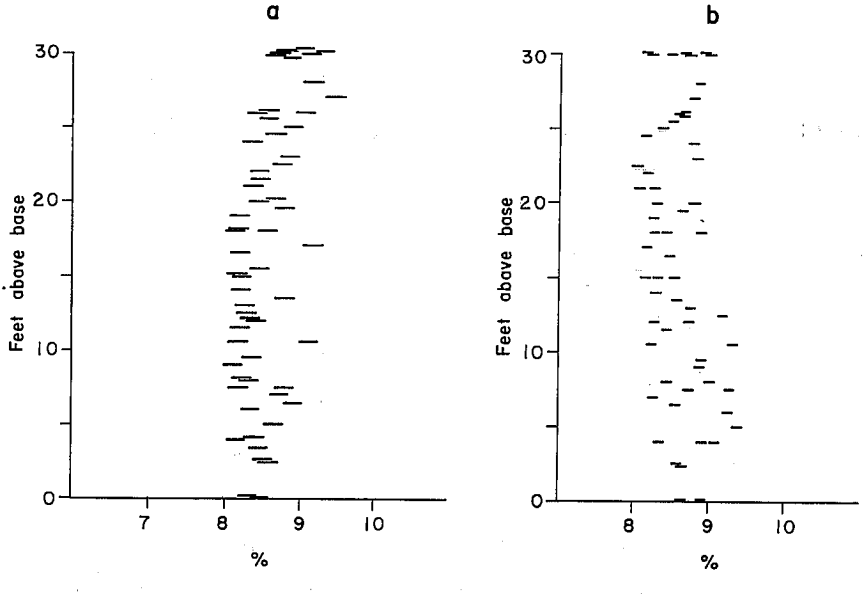

TEXT-FIGURE 10.—Composite plots for CaO (a) and MgO (b).

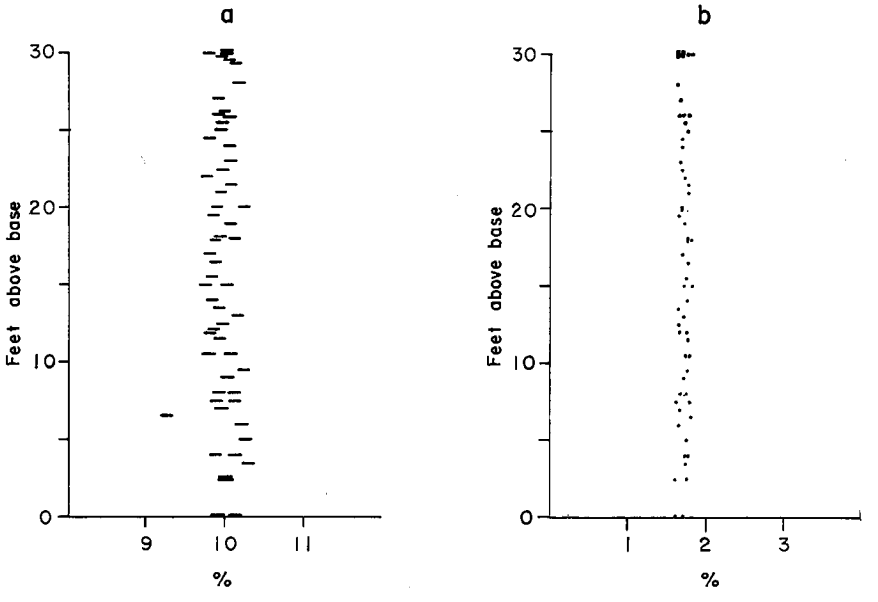

TEXT-FIGURE 11.—Composite plots for FeO (a) and TiO_2 (b)

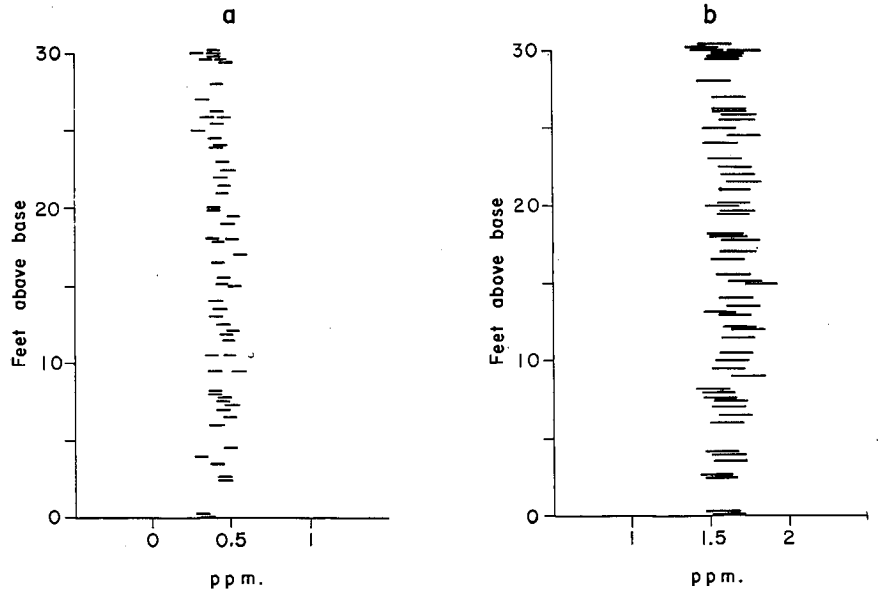

TEXT-FIGURE 12.—Composite plots for U (a) and Th (b).

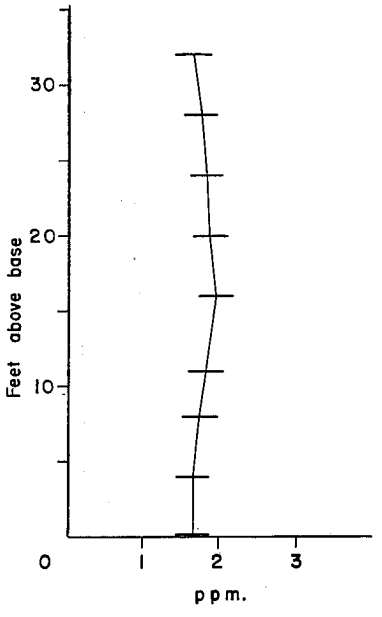

TEXT-FIGURE 13.—Plot of the mean Th values obtained from replicate runs of all samples in section 3. Length of horizontal bars indicates instrumental precision (as standard deviation).

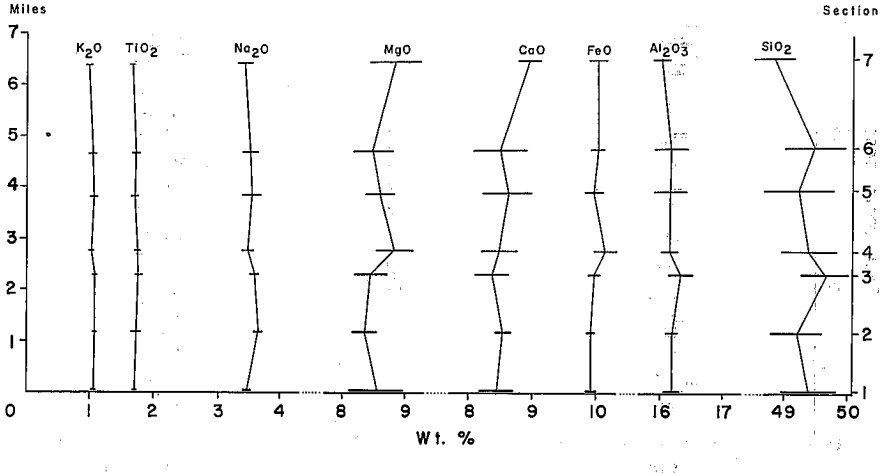

TEXT-FIGURE 14.—Lateral variation in major elements within the Gunlock flow based on mean values for each constituent from each vertical section. Ordinate is approximate distance from the toe of the flow in miles. Length of horizontal bars indicates standard deviation of each constituent from each section.

The variation in Al_2O_3 is much less consistent between individual sections. Overall (Text-fig. 8b) there appears to be essentially no significant variation trends.

Na_2O and K_2O.—Na_2O and K_2O in individual sections as well as the composite sections (Text-fig. 9a and b) show a very weak tendency to decrease in the upper-most part of the flow. Some individual sections also display a weak maximum in the center of the flow.

CaO, MgO, and FeO.—CaO shows a marked tendency, in both individual and composite sections (Text-fig. 10a), toward an increase in the upper half of the flow. The MgO content (Text-fig. 10b) shows the opposite tendency, a decrease in the upper half. Many individual sections also show a marked decrease in both of these constituents toward the center of the flow.

Total Fe (represented as FeO Text-fig. 11a) shows a less extreme but possibly similar variation compared to MgO.

TiO_2.— The variation in TiO_2 is quite irregular in individual sections, but the composite section (Text-fig. 11b) shows an essential uniformity.

U and Th—The real variation in U within the Gunlock flow is quite small; however, like SiO_2, K_2O, and Na_2O, it shows a slight decrease in concentration in the upper portion of the flow, and in some cases, especially in section 3, a decrease near the base. This trend is also reflected in the composite section (Text-fig. 12a).

The variation of Th within this flow is generally below the limits of detection by gamma-ray spectrometry. However, precision was increased by making three to seven replicate determinations for all samples in section 3. The resulting trend (Text-fig. 13) is similar to, although much more distinct than, the trends observed in several other section as well as the composite section (Text-fig. 12b). It is thus evident that there is a significant increase in Th toward the center of the flow. This trend is what would be predicted by the observed variations in K_2O, Na_2O, and U.

As was previously mentioned, lateral variations in the Gunlock flow are much less extreme than vertical variations. No obvious trends are seen in a comparison of section 1 through 6, but if section 7 is included, some trends from the toe of the flow northward are observed (Text-fig. 14). SiO_2, Al_2O_3, K_2O, Na_2O, and TiO_2 all show an increase in concentration toward the toe of the flow (from section 7 to section 1). The opposite trend is seen for MgO, CaO, total Fe, and the Mg/Fe ratio. This variation, if it is real, demonstrates a tendency towards a more mafic bulk composition of the flow towards the source.

Dike-Host Rock Relationships

A sample of the dike rock (HD-1, Table B-1 in Appendix) from a diabase flow of the Hurricane type located approximately one mile north of Cane Springs in northwestern Arizona (See Best, *et al.,* 1969) has been analyzed and compared with the composition of the enclosing diabase (HH-1, Table B-1) in order to determine their chemical relationship. The dike shows, relative to its host, a marked increase in the concentration of Na_2O, K_2O, total Fe, TiO_2, Th, and U with a corresponding decrease in Al_2O_3, MgO, CaO, and the Mg/Fe and Fe/Ti ratios. The SiO_2 in the dike shows only a slight increase over that in the host rock. This data supports other evidence cited earlier that the dike resulted

from crystallization of a late liquid differentiate derived from the surrounding diabase.

IMPLICATIONS OF OBSERVED VARIATIONS

Sampling for Comparative Chemical Studies

The real, but small, variation found within the Gunlock flow indicates that a single sample of basalt may not be representative of the whole flow. The need for the use of more objective sampling techniques thus becomes apparent and is even more critical when the much greater variations found by Watkins and co-workers and Taylor (1966) are considered.

Watkins, *et al.* (1967), Gunn, *et al.* (1968), and Watkins and Gunn (1969), have reported critically large vertical variations in major and trace element concentrations as well as oxidation indices in an Icelandic tholeiite (Table IV). Reported variations were generally several times those found in the Gunlock flow (compare Table II, fifth column, and Table IV) and would have a profound effect on interflow comparisons. These workers conclude that the problem of obtaining representative chemical samples is considerable and Watkins and Gunn (1969, p. 86) suggest that only samples containing "unquenched low oxidation state titanomagnetites" be used for analyses.

Taylor (1966) has analyzed 12 samples along the length of a recent 18 km flow in the central Cascade Range of Oregon. This flow changes from a basaltic andesite (60 percent SiO_2) at the source to an olivine basalt (52 percent SiO_2) at the terminus. Lateral variation of this magnitude would definitely necessitate extensive sampling of a single flow to assure a representative composition.

Although the data obtained in this study of the Gunlock flow indicates that not all flows show the extreme variation reported by Watkins and associates and by Taylor, it is evident that care must be taken in sampling basalt flows for comparative chemical studies. The type of variation within the Gunlock, as well as Icelandic and Cascade flows, indicates that the best technique for obtaining representative samples would be to take at least three or four samples from

TABLE IV

Vertical chemical variation in an Icelandic tholeiite flow 30 feet thick

	min.	max.	mean	s	max. error
SiO_2	44.90	47.40	——	——	0.5
Al_2O_3	15.3	16.8	——	——	0.5
Fe	11.00	12.15	——	——	0.05
CaO	11.4	12.9	——	——	0.05
K_2O	0.223	0.480	——	——	0.005
TiO_2	1.78	2.15	——	——	0.005
Th	0.20	4.32	1.14	1.14	0.40
U	0.13	4.20	0.64	1.12	0.36
Th/U	0.95	5.10	2.68	1.44	——

Data on major elements from Gunn, *et al.* (1968) and for Th, U and Th/U from Watkins, *et al.* (1967). All elemental values are in weight percent except Th and U which are in ppm. Maximum error is maximum experimental error. Note the relatively large s for Th and U.

three or more vertical sections, widely spaced, along the length of the flow. When possible, the vesicular and often weathered tops and bottoms of flows should be avoided in sampling. It is realized that in the case of recent flows such as that sampled by Taylor, only the upper crust of the flow is available to sampling. In these cases, it seems essential that several samples be taken at intervals along the length of the flow.

Sampling techniques such as those mentioned above would not only assure a more representative mean composition for the flow analyzed, but would also provide much needed data for a better understanding of the magnitude and types of variations that exist within single lava flows.

Classification

Regarding the effect of the chemical variation of the order observed in the Gunlock flow on the classification of basalts in the western Grand Canyon region, a comparison of the data in the last two columns in Table II discloses that variation in the Gunlock flow is less for any constituent than the least variation found within any basalt type in the region (Best, *et al.*, 1969, Table 2). Regional variations are two to twenty times those in the Gunlock flow.

The Gunlock flow as a whole is slightly nepheline-normative. In spite of this, a few of the individual samples (Tables B-II through B-VIII in Appendix) are slightly hypersthene-normative, and since Gunlock samples thus straddle the critical plane of silica saturation (Yoder and Tilley, 1962) with either nepheline or hypersthene in the norm, they also stradle the critical difference between an alkali olivine basalt and an olivine tholeiite. In this respect, however, the Gunlock flow is somewhat of a special case and for the majority of flows in the Grand Canyon region, variation of this magnitude in the norm would not appreciably affect the classification.

As the appearance of hypersthene in the norm shows an apparent relationship to the position of the sample in the flow, generally being found near the center, it would seem that the best sampling techniques to avoid inaccurate classification would be to collect several samples vertically through the flow.

Some vertical and lateral modal variation apparently exists within the Gunlock flow. However, when compared to the difference in mineralogical composition between major basalt types in this region (Best, *et al.*, 1969), these variations are not significant enough to affect the classifiaction of an individual flow for interflow comparisons.

Evans and Moore (1968) have found that although the bulk of the basalt in the Makaopuhi lava lake, Hawaii, is tholeiitic the mode of the upper chill zone has an "alkali basalt flavor." They have expressed concern over the possibility of getting an inaccurate impression of the nature of a body of basalt by only sampling the top. Although it seems unlikely that such extreme modal variations as are developed in the 225 foot-thick Makaopuhi lava lake would be present in the average basalt flow, it is evident that, at least in some cases, significant modal variations do exist. J.G. MacDonald (1967) has found two to four times as much modal variation in a Scottish flow as was found in the Gunlock flow, and Taylor (1966) reports a variation of 15 percent in the phenocrystic plagioclase of a flow in Oregon. Modal variations of this magnitude would present problems in classification, and stress the advantage of using a chemical or normal classification scheme.

PETROLOGIC INTERPRETATIONS

Summary of Pertinent Data

The following general conclusions can be drawn concerning the variations within the Gunlock flow:

1) Modal plagioclase shows an overall tendency to decrease upward in two sections. There is a poorly defined tendency toward an upward increase in the minimum An content of the grains in one section.

2) Modal olivine is quite variable, showing an upward increase in section 6 and a decrease in section 3.

3) Modal pyroxene has a maximum over a minimum at the center of both of two vertical sections. Section 3 shows an upward increase, while section 6 increases toward the center.

4) Fe-Ti Oxide phases show no consistent modal variation but show a definite increase in oxidation index toward the lower center of the flow. A plot of the oxidation index verses the position in the flow (Text-fig. 5) corresponds closely to similar plots for Icelandic flows (Watkins and Haggerty, 1967). The degree of oxidation seems to be related to the temperature distribution after a period of cooling (Text-fig. 6).

5) Although the modal variations in the two sections examined are not consistent, the overall upward decrease in plagioclase in both sections, the upward increase in pyroxene in section 3 and in olivine in section 6, along with the irregular variation in the oxides, are similar to, though less pronounced than, the trends observed in a Scottish flow by J.G. MacDonald (1967).

6) SiO_2, Na_2O, K_2O, U, and Th all show a decrease in the upper portion of the flow, and in some cases, a poorly defined decrease at the base. MgO, and to a lesser degree FeO, show a decrease in the upper part of the flow, and in some cases, a poorly defined decrease at the center is superimposed on this trend. CaO increases in the upper part, but also may show a decrease toward the center.

7) The first six vertical sections show no definite and consistent trends in lateral variation. However, if section 7 is added, there is a slight increase in SiO_2, Al_2O_3, Na_2O, K_2O, and TiO_2 and a decrease in MgO, CaO, FeO, and the Mg/Fe from the source toward the toe of the flow.

8) Dikes show a marked enrichment in Na_2O, K_2O, FeO, TiO_2, Th, and U relative to the host rock. There is a corresponding impoverishment in MgO, CaO, and the Mg/Fe and Fe/Ti ratios. Only a slight increase in SiO_2 is evident.

Chemical Variations

Although well beyond analytical errors, the chemical variations observed in the Gunlock flow are for the most part, small and not entirely consistent, making interpretations hazardous.

Lateral Variation.— There are three major problems in interpreting lateral variations within the Gunlock flow.

(1) Sampled sections represent only a one-dimensional sequence along the inverted valley with no reliable control on transverse variation. This sampling problem is not serious, however, because the flow is essentially one-dimensional

anyway and represents a narrow river of lava rather than a broad sheet or flood of basalt.

(2) The exact mechanisms involved in extrusion and flow are not understood. J.G. MacDonald (1967, p. 44) calls upon a mechanism by which "earlier erupted material, cooling from the base," is "overridden by the later fractions which gradationally build up successive layers", while G.A. MacDonald (1967, p. 17) states that lava flows are fed by a narrow surface stream of lava (occupying only a fraction of the width of the flow) which breaks up into numerous subcrustal distributaries to feed the advancing front. In this case the majority of the flow crusts over rapidly and solidification proceeds dominantly from the top down rather than from the base up as suggested by J.G. MacDonald (1967).

(3) There is some hesitancy in including sample section 7 with the first 6 for it is located north of the area where the flow is comprised of multiple flow units and an unequivocal correlation across this complex area is not possible.

In spite of these problems, if substantial lateral variation exists, such as that found by Taylor (1966) in Oregon, within the Gunlock flow, it would have been detected. The variation observed between seven vertical sections is so small and inconsistent as to preclude detailed interpretation and to a first approximation it may be stated that no significant lateral variation in chemical composition exists within the part of the flow sampled.

Vertical Variation.— Vertical chemical variations in a basalt flow could be created by (1) inhomogeneity of the erupting magma related to pre-eruptive processes within the magma chamber, (2) eruptive processes, including flow mechanisms both within the chamber and conduit and on the surface after extrusion, and (3) post-eruptive or post-emplacement processes which would include differentiation during cooling and weathering or alteration after cooling.

Since essentially no lateral variation exists within the Gunlock flow as sampled, it is evident that any vertical variation present could not be due to pre-eruptive processes. Flow during the eruption, on the other hand, could have produced some inhomogeneity by flowage differentiation of phenocrysts (compare Gibb, 1968). As the mechanism of flow is not understood it is not warranted here to evaluate possible inhomogeneities of this kind.

Let us suppose that most of the existing vertical variation is the result of post-emplacement processes.

Since most of the chemical variation is the opposite of what would be expected as the result of weathering (Rankama and Sahama, 1950, p. 193) the vertical variation observed cannot be explained by this process.

Regarding processes of differentiation, settling of olivine phenocrysts could have occurred in the slower cooling, central and lower parts of the flow. However, the modal data does not clearly support this process.

Loss of alkalies from the top of the flow with the escaping vapor phase is a possible explanation for the decrease in K_2O and Na_2O at the top of the flow. In this connection Richter and Moore (1966) demonstrated the existence of a transient zone of alkali enrichment just below the solidifying crust of the Kilauea Iki lava lake, Hawaii. This zone was apparently produced by temporary fixation of the alkalies from the ascending volatile phase and was not found in the rock after solidification. There is also a possibility of some SiO_2 escaping in this manner, but this was not proven.

The slight central enrichment of SiO_2, Na_2O, K_2O, U, and Th, in the Gunlock flow and the corresponding impoverishment of CaO, MgO, and possibly FeO might be explained by differential diffusion of ions in the liquid portion of the lava. Wager, *et al.* (1960, p. 77) and Jackson (1961, p. 61, 62) for example have described diffusion of this type in connection with adcumulus growth in crystal mushes resting on the floors of layered intrusions. This process produces extreme rock compositions (*i.e.* mono- and bi-mineralic dunites, peridotites, etc.) from magmas of basaltic composition by migration of Ca, Mg, and Fe to cumulate crystals and accompanying expulsion of Na, K, and Si to the overlying liquid. Admittedly, the cooling time of a lava flow is many orders of magnitude less than that of large layered intrusions, but conceivably a very slight amount of detectable diffusion could take place producing the observed vertical variations. The base and top (by inversion) of the lava flow would have analogous relations to the floor of layered intrusions.

It is obvious from the inconsistency and variety of variation observed that more than one mechanism may have been responsible for the observed data, and although others may well exist, some or all mechanisms mentioned above present the best possible interpretations at this time.

APPENDIX A

TABLE A-I

Modal compositions in volume percent for each sample in vertical sections 3 and 6 and for the dike rock from the Gunlock flow (GD). The mean and standard deviation (s) for each mineral throughout the two sections are indicated, as is the calculated counting error for each mineral (Soloman, 1963).

	Modal Data				
	Pl	Px	Ol	Ox	Ap
Errors	0.50	0.30	0.96	0.05	——
3-32	——	——	10.35	——	——
3-28	57.3	22.9	18.2	1.6	——
3-24	60.4	24.9	13.0	1.6	——
3-20	59.4	26.3	11.7	2.7	——
3-16	64.1	20.1	14.8	1.4	——
3-11	62.2	20.6	16.3	1.3	——
3-8	61.9	22.1	14.5	1.5	——
3-4	61.3	20.5	16.8	1.3	——
3-0	——	——	13.4	——	——
Mean	60.9	22.5	14.3	1.6	——
s	2.2	2.4	2.5	0.5	——
6-30	——	——	16.16	——	——
6-27	57.9	24.2	15.5	2.4	——
6-24	58.3	25.6	14.2	2.0	——
6-21.5	62.6	26.4	9.3	1.7	——
6-18	56.9	28.6	12.3	2.1	——
6-14	65.7	21.2	9.7	3.5	——
6-11.5	63.0	25.7	8.7	2.8	——
6-8	60.0	25.9	10.0	4.1	——
6-4	60.7	24.3	13.4	1.7	——
6-0	——	——	11.1	——	——

Table A-I (cont.)

	Pl	Px	Ol	Ox	Ap
Mean	60.7	25.2	12.0	2.5	——
s	3.0	2.1	2.7	0.9	——
GD	58.0	25.8	1.2	11.7	3.28

APPENDIX B

TABLE B-I

Grand Wash Flows and Cane Springs Samples

Radioactivities of the three flows in the stream channel northwest of the Veyo cone and chemical compostitions of the dike (HD-1) and host rock (HH-1) from the flow of Hurricane diabase near Cane Springs. Oxides are given in weight percent; Th and U in ppm; total Fe as FeO; and K_2O determinations by both atomic absorption (a) and gamma-ray spectrometry (g) are given. The Fe^{+3}/Fe^{+2} ratio was taken as 0.125 for norm determinations in order to conform with Best, *et al.* (1969). These specifications are the same for Table B-I through B-IX.

Samples	8L	8M	8U	HH-1	HD-1
SiO_2	——	——	——	49.86	50.08
Al_2O_3	——	——	——	16.31	14.36
FeO	——	——	——	10.67	13.40
MgO	——	——	——	6.96	3.54
CaO	——	——	——	9.73	8.33
Na_2O	——	——	——	3.19	3.92
aK_2O	——	——	——	1.00	2.09
gK_2O	0.93	1.08	1.08	0.98	1.94
TiO_2	——	——	——	1.77	3.11
Total	——	——	——	99.48	98.81
Th	1.90	2.11	2.14	2.45	5.58
U	0.36	0.45	0.39	0.33	0.87
Th/U	——	——	——	7.42	6.41
Mg/Fe	——	——	——	0.52	0.21
Fe/Ti	——	——	——	7.62	5.46
Qz	——	——	——	0.0	0
Or	——	——	——	6.11	12.61
Pl	——	——	——	55.31	45.16
AnPl	——	——	——	49.72	33.94
Ne	——	——	——	0.0	2.04
Hy	——	——	——	3.08	0
Ol	——	——	——	12.28	9.62
Mt	——	——	——	1.92	2.38
Il	——	——	——	3.47	6.00
Di	——	——	——	17.79	22.16

TABLE B-II

Chemical compositions and norms for all samples in section 1.

Samples	1-5	1-8	1-10.5	1-12.5	1-15.5	1-19
SiO_2	49.86	49.54	49.65	49.65	48.90	48.79
Al_2O_3	16.10	16.03	16.25	16.18	16.41	16.16
FeO	9.92	9.98	9.87	9.89	9.79	10.01
MgO	9.00	9.18	8.48	8.30	8.15	8.15
CaO	8.22	8.26	8.19	8.44	8.65	8.86
Na_2O	3.56	3.40	3.43	3.46	3.42	3.46
aK_2O	1.02	1.01	1.04	1.09	1.08	1.04
gK_2O	1.02	1.01	1.01	1.07	1.02	1.04
TiO_2	1.67	1.64	1.74	1.67	1.67	1.67
Total	99.35	99.04	98.66	98.68	98.16	98.14
Th	1.60	1.64	1.71	1.80	1.95	1.47
U	0.46	0.45	0.42	0.40	0.40	0.39
Th/U	3.51	3.64	4.07	4.50	4.88	3.77
Mg/Fe	0.70	0.71	0.67	0.65	0.65	0.63
Fe/Ti	7.71	7.92	7.38	7.69	7.61	7.78
Qz	0	0	0	0	0	0
Or	6.12	6.22	6.46	6.61	6.57	6.34
Pl	54.61	55.77	56.55	54.99	54.27	54.69
AnPl	45.06	46.41	46.59	45.95	48.38	48.34
Ne	0.23	0	0	0	0.83	1.43
Hy	0	0.64	2.23	0	0	0
Ol	21.01	19.16	16.93	19.68	19.34	19.03
Mt	1.79	1.86	1.84	1.80	1.79	1.83
Il	3.20	3.23	3.44	3.23	3.25	3.24
Di	13.00	13.08	12.51	13.66	13.91	15.39

TABLE B-III

Chemical compositions and norms for all samples in section 2.

Samples	2-2	2-5.5	2-9	2-12	2-16	2-20	2-23
SiO_2	49.11	49.65	49.86	48.68	49.01	49.01	49.01
Al_2O_3	16.14	16.06	16.31	16.16	16.20	16.25	16.31
FeO	10.00	9.96	9.84	9.84	9.93	9.88	9.88
MgO	8.58	8.27	8.27	8.15	8.27	8.67	8.22
CaO	8.50	8.71	8.40	8.43	8.36	8.57	8.64
Na_2O	3.64	3.63	3.73	3.58	3.70	3.62	3.58
aK_2O	1.06	1.07	1.10	1.06	1.08	1.03	1.08
gK_2O	1.06	1.04	1.08	1.02	1.04	0.99	1.02
TiO_2	1.60	1.65	1.72	1.72	1.74	1.70	1.80
Total	98.63	99.00	99.23	97.61	98.27	98.72	98.51
Th	1.64	1.72	1.90	1.80	1.81	1.87	1.94
U	0.46	0.45	0.47	0.45	0.44	0.35	0.39
Th/U	3.57	3.79	4.06	4.00	4.11	5.34	4.97
Mg/Fe	0.67	0.64	0.65	0.64	0.65	0.68	0.64
Fe/Ti	8.09	7.82	7.43	7.43	7.42	7.53	7.11
Qz	0	0	0	0	0	0	0
Or	6.38	6.43	6.64	6.45	6.56	6.24	6.54
Pl	51.98	52.63	53.58	53.32	52.45	52.08	52.72
AnPl	46.98	45.88	45.24	46.95	46.46	47.84	47.73
Ne	2.05	1.42	1.36	1.51	2.09	2.13	1.77
Hy	0	0	0	0	0	0	0
Ol	20.06	18.94	19.18	19.35	19.48	20.00	19.04
Mt	1.82	1.81	1.78	1.81	1.82	1.80	1.80
Il	3.10	3.18	3.30	3.36	3.37	3.29	3.49
Di	14.58	15.55	14.13	14.15	14.20	14.43	14.60

TABLE B-IV

Chemical compositions and norms for all samples in section 3.

Samples	3-0	3-4	3-8	3-11	3-16	3-20	3-24	3-28	3-32
SiO_2	49.22	49.65	49.86	50.18	49.86	49.86	49.43	49.82	48.96
Al_2O_3	16.52	16.56	16.41	16.58	16.31	16.16	16.27	16.29	15.97
FeO	9.92	9.87	9.89	9.80	10.02	10.06	9.96	10.03	10.03
MgO	8.63	8.33	8.73	8.25	8.30	8.25	8.02	8.65	8.75
CaO	8.46	8.12	8.16	8.18	8.15	8.19	8.74	8.40	8.79
Na_2O	3.52	3.62	3.70	3.58	3.58	3.54	3.46	3.56	3.54
aK_2O	1.04	1.06	1.09	1.09	1.10	1.07	1.04	1.04	1.03
gK_2O	1.00	0.98	1.04	1.03	1.07	1.02	1.03	1.01	1.00
TiO_2	1.70	1.77	1.79	1.79	1.80	1.70	1.67	1.75	1.67
Total	99.01	98.98	99.63	99.44	99.13	98.83	98.59	98.74	98.74
Th	1.66	1.66	1.75	1.82	1.96	1.88	1.83	1.76	1.66
U	0.35	0.49	0.50	0.49	0.53	0.48	0.48	0.46	0.46
Th/U	4.70	3.42	3.52	3.70	3.75	3.93	3.83	3.86	3.65
Mg/Fe	0.67	0.65	0.68	0.65	0.64	0.64	0.62	0.67	0.68
Fe/Ti	7.56	7.24	7.19	7.12	7.21	7.76	7.74	7.43	7.80
Qz	0	0	0	0	0	0	0	0	0
Or	6.29	6.37	6.53	6.70	6.81	6.60	6.32	6.25	6.23
Pl	54.08	56.06	54.13	57.43	56.93	56.58	54.76	54.44	51.03
AnPl	47.95	45.65	45.31	45.60	44.87	45.02	46.89	45.91	47.98
Ne	1.11	0.30	1.01	0	0	0	0.36	0.50	2.07
Hy	0	0	0	1.39	0.07	1.24	0	0	0
Ol	20.40	20.10	20.36	16.84	17.86	17.10	18.93	20.23	19.90
Mt	1.80	1.79	1.78	1.81	1.86	1.87	1.81	1.81	1.83
Il	3.28	3.41	3.42	3.51	3.56	3.37	3.23	3.36	3.22
Di	13.01	11.94	12.73	12.29	12.88	13.20	14.56	13.37	15.68

TABLE B-V

Chemical compositions and norms for all samples in section 4.

Samples	4-3	4-5	4-8	4-11	4-15	4-17	4-21	4-25
SiO_2	49.11	49.33	49.65	50.29	49.43	48.79	49.22	49.22
Al_2O_3	16.29	16.24	16.12	16.24	16.05	15.91	16.16	16.27
FeO	10.30	10.21	10.23	10.15	10.11	10.24	9.91	9.78
MgO	9.06	9.25	8.90	8.75	8.88	8.80	8.37	8.47
CaO	8.44	8.33	8.33	8.23	8.11	8.68	8.88	8.79
Na_2O	3.42	3.58	3.54	3.55	3.54	3.35	3.36	3.39
aK2O	0.95	0.99	1.02	1.05	1.00	0.96	0.95	0.96
TiO_2	1.72	1.64	1.75	1.70	1.79	1.67	1.72	1.74
Total	99.36	99.56	99.55	99.97	98.85	98.42	98.61	98.64
Th	1.74	1.70	1.72	1.81	1.69	1.66	1.62	1.68
U	0.41	0.40	0.40	0.40	0.39	0.39	0.30	0.28
Th/U	4.25	4.28	4.27	4.02	4.33	4.26	5.32	6.00
Mg/Fe	0.68	0.70	0.67	0.67	0.68	0.67	0.65	0.67
Fe/Ti	7.78	8.10	7.57	7.74	7.63	7.96	7.48	7.31
Qz	0	0	0	0	0	0	0	0
Or	5.98	5.97	6.18	6.46	6.16	5.96	6.03	5.96
Pl	53.59	52.68	53.85	56.27	54.40	52.91	54.29	54.57
AnPl	48.24	47.31	45.83	45.11	45.43	47.98	47.76	47.94
Ne	0.77	1.47	0.51	0	0.37	0.71	0.30	0.41
Hy	0	0	0	0.87	0	0	0	0
Ol	21.56	21.74	20.90	18.11	21.23	20.70	19.32	19.53
Mt	1.86	1.84	1.84	1.87	1.84	1.87	1.81	1.78
Il	3.30	3.13	3.35	3.33	3.32	3.23	3.33	3.36
Di	12.90	13.13	13.32	13.06	12.65	14.58	14.90	14.36

TABLE B-VI

Chemical compositions and norms for all samples in section 5.

Samples	5-3	5-7	5-10	5-13	5-16.5	5-20	5-24	5-28	5-31	5-33
SiO_2	49.43	49.22	49.22	48.79	49.86	49.22	49.65	49.86	48.58	48.15
Al_2O_3	16.20	15.88	16.06	16.05	16.44	16.33	16.63	16.29	15.84	15.89
FeO	10.00	9.27	10.02	9.82	9.74	9.91	9.76	9.93	10.14	10.01
MgO	8.65	8.55	8.86	8.72	8.52	8.27	8.17	8.50	8.85	8.67
CaO	8.57	8.90	8.09	8.32	8.19	8.54	8.44	8.55	9.14	9.30
Na_2O	3.54	3.56	3.64	3.64	3.71	3.60	3.52	3.50	3.31	3.24
aK_2O	1.01	1.07	1.08	1.06	1.12	1.09	1.09	1.06	0.95	0.95
gK_2O	0.99	1.06	1.10	1.06	1.07	1.07	1.02	1.01	0.90	0.92
TiO_2	1.75	1.80	1.70	1.64	1.70	1.72	1.70	1.70	1.60	1.60
Total	99.14	98.95	98.69	98.03	99.28	98.68	98.97	99.39	98.41	97.81
Th	1.58	1.82	1.99	2.00	2.18	1.72	1.88	1.83	1.54	1.56
U	0.46	0.49	0.55	0.51	0.45	0.51	0.43	0.41	0.41	0.38
Th/U	3.48	3.70	3.62	3.92	4.84	3.37	4.37	4.46	3.76	4.11
Mg/Fe	0.67	0.66	0.69	0.69	0.68	0.65	0.65	0.66	0.68	0.67
Fe/Ti	7.40	7.18	7.64	7.79	7.42	7.48	7.44	7.57	8.21	8.10
Qz	0	0	0	0	0	0	0	0	0	0
Or	6.07	6.44	6.53	6.42	6.71	6.60	6.58	6.34	5.75	5.78
Pl	53.51	50.79	52.81	52.14	54.20	53.12	55.67	54.68	51.10	50.99
AnPl	49.89	47.15	45.69	46.60	45.40	47.04	46.91	46.29	49.91	51.22
Ne	1.01	2.00	1.43	1.98	1.15	1.53	0.36	0.26	1.59	1.76
Hy	0	0	0	0	0	0	0	0	0	0
Ol	20.04	18.95	20.97	20.35	19.94	19.33	19.46	19.80	20.13	19.67
Mt	1.81	1.81	1.82	1.80	1.76	1.80	1.77	1.80	1.85	1.84
Il	3.37	3.47	3.29	3.18	3.27	3.32	3.28	3.27	3.11	3.13
Di	14.15	16.51	13.11	14.10	12.93	14.25	12.84	13.81	16.44	16.80

TABLE B-VII

chemical compositions and norms for all samples in section 6.

Samples	6-0	6-4	6-8	6-11.5	6-14	6-18	6-21.5	6-24	6-27	6-30
SiO_2	49.43	49.43	49.22	49.97	49.86	49.86	50.08	49.43	48.90	48.58
Al_2O_3	16.06	16.16	16.56	16.52	16.24	16.24	16.27	16.06	15.69	15.88
FeO	10.12	10.12	10.10	9.91	9.84	9.88	10.06	10.03	9.89	10.06
MgO	8.90	8.90	8.45	8.43	8.28	8.42	8.08	8.78	8.78	9.00
CaO	8.30	8.40	8.30	8.20	8.20	8.16	8.43	8.33	9.46	9.02
Na_2O	3.50	3.59	3.51	3.70	3.52	3.58	3.59	3.44	3.29	3.35
aK_2O	0.98	0.98	1.02	1.08	1.06	1.04	1.10	0.96	0.95	0.94
gK_2O	0.93	0.95	0.99	1.06	1.02	1.01	1.08	0.93	0.93	0.92
TiO_2	1.60	1.72	1.74	1.75	1.74	1.74	1.75	1.67	1.65	1.59
Total	98.90	99.30	98.90	99.57	98.74	98.91	99.37	98.71	98.62	99.40
Th	1.71	1.71	1.53	1.85	1.82	1.84	1.93	1.62	1.74	1.40
U	0.32	0.31	0.40	0.48	0.40	0.42	0.46	0.42	0.32	0.43
Th/U	5.34	5.52	3.82	3.89	4.55	4.38	4.20	3.86	5.44	3.26
Mg/Fe	0.68	0.68	0.65	0.66	0.65	0.66	0.62	0.68	0.69	0.69
Fe/Ti	8.20	7.64	7.55	7.33	7.36	7.38	7.45	7.80	7.77	8.23
Qz	0	0	0	0	0	0	0	0	0	0
Or	5.94	5.91	6.15	6.47	6.53	6.45	6.63	5.95	5.73	5.68
Pl	54.28	53.31	55.33	54.97	56.76	57.04	55.03	56.39	50.79	51.25
AnPl	46.13	46.46	47.35	45.31	45.42	44.84	44.88	46.17	49.38	49.69
Ne	0.41	1.16	0.53	0.79	0	0	0.17	0	1.42	1.68
Hy	0	0	0	0	1.75	0.39	0	0.54	0	0
Ol	21.22	20.80	20.55	19.95	16.68	17.82	19.13	18.52	19.04	20.51
Mt	1.84	1.83	1.84	1.79	1.83	1.84	1.82	1.87	1.80	1.84
Il	3.09	3.30	3.35	3.36	3.43	3.43	3.36	3.31	3.20	3.08
Di	13.18	13.65	12.22	12.65	12.98	12.98	13.82	13.39	17.99	15.94

TABLE B-VIII

Chemical compositions and norms for all samples in section 7.

Samples	7-5	7-7.5	7-10.5	7-13.5	7-17	7-19.5	7-23	7-26	7-30
SiO_2	48.58	49.01	49.01	49.22	49.01	48.79	48.58	49.01	48.15
Al_2O_3	15.88	15.91	15.86	16.20	16.08	15.97	15.99	16.10	16.08
FeO	10.28	10.11	10.06	9.91	9.80	9.84	10.05	9.98	9.92
MgO	9.38	9.26	9.30	8.55	8.18	8.63	8.81	8.58	8.91
CaO	8.65	8.79	9.10	8.79	9.17	8.78	8.85	9.02	9.11
Na_2O	3.29	3.40	3.46	3.56	3.56	3.54	3.38	3.46	3.24
aK_2O	0.95	0.91	0.97	1.02	1.02	1.02	0.95	0.96	0.88
gK_2O	——	0.89	0.95	0.99	0.98	0.99	0.90	0.93	0.84
TiO_2	1.75	1.60	1.72	1.62	1.67	1.62	1.64	1.64	1.60
Total	98.76	99.00	99.47	98.88	98.50	98.19	98.24	98.74	97.90
Th	——	1.61	1.79	1.94	1.85	1.80	1.70	1.75	1.72
U	——	0.45	0.38	0.43	0.56	0.51	0.45	0.42	0.34
Th/U	——	3.58	4.71	4.51	3.30	3.53	3.78	4.13	5.04
Mg/Fe	0.71	0.71	0.72	0.67	0.65	0.68	0.68	0.67	0.70
Fe/Ti	7.61	8.19	7.59	7.94	7.62	7.89	7.97	7.92	8.03
Qz	0	0	0	0	0	0	0	0	0
Or	5.72	5.49	5.83	6.15	6.18	6.20	5.75	5.80	5.34
Pl	52.23	52.31	49.81	52.42	51.18	51.42	52.37	52.19	52.58
AnPl	48.89	48.19	49.25	47.63	48.40	47.96	48.94	48.74	50.98
Ne	0.85	1.10	2.27	1.68	2.32	2.05	1.30	1.60	1.24
Hy	0	0	0	0	0	0	0	0	0
Ol	21.73	21.19	20.34	19.57	18.16	19.67	20.40	19.55	20.48
Mt	1.87	1.83	1.82	1.80	1.79	1.80	1.84	1.82	1.82
Il	3.38	3.08	3.30	3.12	3.23	3.14	3.17	3.16	3.12
Di	14.18	14.95	16.60	15.22	17.11	15.68	15.14	15.85	15.39

TABLE B-IX

Mean chemical compositions, standard deviations, and norms for sample sections 1 through 7. The mean of all sections combined is Gun.

Samples	1		2		3		4		5		6		7		Gun	
SiO_2	49.40	0.44	49.19	0.41	49.65	0.38	49.38	0.44	49.20	0.56	49.48	0.48	48.82	0.33	49.30	0.27
Al_2O_3	16.19	0.13	16.20	0.09	16.34	0.20	16.16	0.13	16.16	0.26	16.17	0.27	16.01	0.12	16.18	0.10
FeO	9.91	0.08	9.90	0.06	9.95	0.09	10.12	0.18	9.93	0.13	10.00	0.11	9.99	0.15	9.97	0.08
MgO	8.54	0.44	8.35	0.20	8.43	0.26	8.81	0.29	8.58	0.23	8.60	0.31	8.84	0.41	8.59	0.18
CaO	8.44	0.27	8.52	0.13	8.35	0.26	8.47	0.28	8.60	0.40	8.48	0.42	8.92	0.18	8.54	0.18
Na_2O	3.46	0.06	3.64	0.06	3.57	0.07	3.47	0.10	3.53	0.15	3.51	0.12	3.43	0.12	3.52	0.07
aK_2O	1.05	0.03	1.07	0.02	1.06	0.03	1.01	0.03	1.05	0.06	1.01	0.06	0.96	0.05	1.03	0.04
gK_2O	1.03	0.02	1.04	0.03	1.02	0.03	0.98	0.04	1.02	0.07	0.98	0.06	0.93	0.05	1.00	0.04
TiO_2	1.68	0.03	1.71	0.07	1.74	0.05	1.72	0.05	1.69	0.06	1.70	0.06	1.65	0.05	1.70	0.03
Total	98.67		98.58		99.09		99.14		98.74		98.95		98.62		99.09	
Th	1.70	0.17	1.81	0.10	1.78	0.11	1.70	0.06	1.81	0.21	1.72	0.16	1.77	0.10	1.76	0.05
U	0.42	0.03	0.43	0.04	0.47	0.05	0.37	0.05	0.46	0.05	0.40	0.06	0.44	0.07	0.43	0.03
Th/U	4.06	0.53	4.26	0.63	3.82	0.37	4.59	0.70	3.96	0.47	4.43	0.78	4.07	0.63	4.17	0.27
Mg/Fe	0.67	0.03	0.65	0.02	0.66	0.02	0.67	0.01	0.67	0.01	0.67	0.02	0.69	0.02	0.67	0.01
Fe/Ti	7.68	0.18	7.55	0.32	7.44	0.25	7.70	0.26	7.62	0.33	7.67	0.33	7.86	0.21	7.65	0.13
Qz	0		0		0		0		0		0		0		0	
Or	6.31		6.46		6.36		6.06		6.30		6.07		5.81		6.23	
Pl	54.57		52.55		54.76		53.90		52.80		54.32		51.85		53.46	
AnPl	46.52		46.71		45.96		46.88		47.27		46.36		48.82		46.93	
Ne	0.35		1.81		0.56		0.57		1.37		0.51		1.60		1.01	
Hy	0		0		0		0		0		0	0				
Ol	20.15		19.42		19.93		20.71		19.89		20.20		20.14		20.05	
Mt	1.80		1.80		1.80		1.83		1.81		1.81		1.82		1.81	
Il	3.26		3.32		3.34		3.31		3.25		3.28		3.20		3.29	
Di	13.52		14.60		13.22		13.57		14.54		13.76		15.55		14.12	